

Dear editor,

Please find our responses to the referee comments (**bold**) below, along with the relevant amendments to the manuscript (*italics*).

The manuscript has been modified according to the comments, including:

- An augmented discussion about limitations and directions for future implementation in large-scale LSMs, in line with various comments from both referees.
- Description of an additional set of sensitivity simulations to better understand the effect of the key snow parameter ( $H_{Smin}$ ), as suggested by referee #1. See figure in the response below.
- A thorough revision of the text to improve readability and remove grammatical errors, as suggested by referee #2.

Thank you for your consideration of our revised manuscript for publication in The Cryosphere.

On behalf of the authors,  
Kjetil Aas

## Anonymous Referee #1

This paper describes how small-scale surface heterogeneity due to excess ice can be, in a relatively simple way, implemented in land surface models, in this case, the NOAHMP LSM. A companion paper described a similar work with the Cryogrid model. The motivation of the work is clearly and convincingly laid out, the paper is well structured, easy to read and generally well written (except for frequent systematic grammatical errors). The spirit of the paper is that this work should be seen as a proof of concept, and it is made rather clear that the implementation of such an approach in ESMs will not be an easy task.

The methods are described very clearly, and they appear to me appropriate in terms of complexity in the sense that the proposed scheme appears to be on a similar level of complexity as the rest of the model this scheme was implemented in. One might wonder whether some effort should have been devoted to implementing excess ice formation; the possible long time scales involved in the excess ice aggradation could be an argument to discard that option, given that the type of models this approach is designed for is made for centennial-scale simulations, at best.

We agree that it would be desirable to be able also simulate excess ice formation. However, in addition to the long time scales noted above, the processes behind excess ice formation at the two locations are very different, and a unified method for simulating excess ice formation has therefore not yet revealed itself.

The discussion of the limitations of this work is honest. I would have liked to see a more thorough analysis of the sensitivity of the model to some critical parameters, in particular those linked to snow; maybe some sensitivity tests might be in order.

Thank you for this suggestion. We performed a set of simulations to explore the key snow parameter further, which we now describe in the text (section 4.1). See also Fig I.

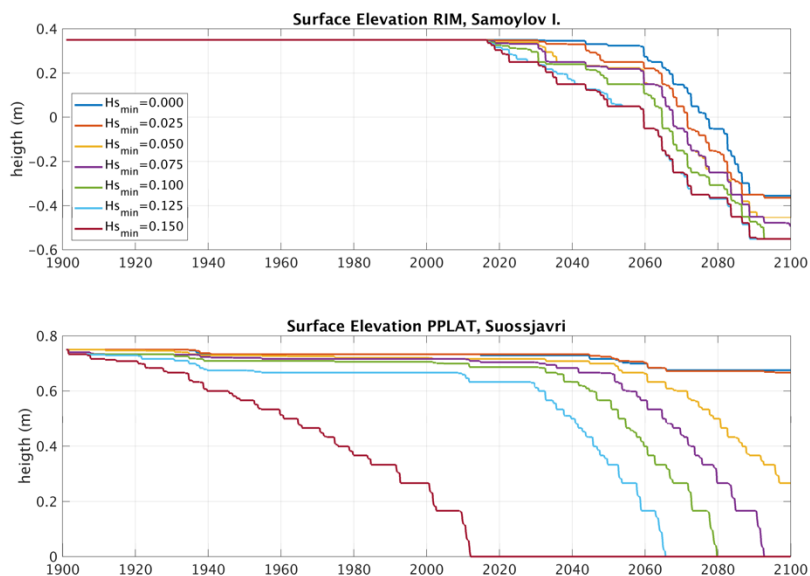


Figure I: Surface elevation of RIM relative to CENTER at Samoylov Island, Siberia (a), and of PPLAT relative to MIRE at Suossjavri, Northern Norway (b) for different values of  $H_{smin}$ .

*An additional set of sensitivity simulations with different values of  $H_{smin}$  ranging from 0.0 to 0.15 m (not shown) revealed that the landscape evolution at the polygonal site was relatively insensitive to this value, with the transition from LCP to HCP shifting by less than two decades between the minimum and maximum value. A larger sensitivity was seen for the peat plateau site, for which the lowest values of  $H_{smin}$  resulted in stable permafrost throughout the 21st century.*

**In the discussion (sections 5.1 and 5.2), it would have been good to provide the reader with some more quantitative (if possible) estimates of the importance of neglected processes, and with corresponding priorities in future developments.**

Thank you for this suggestion. We have now added several points to the discussion about limitations, including reference to the snow sensitivity simulations, discussion of the effect of standing water and our opinion on priorities for further developments.

*Simulating surface water in low-centered polygons, or water-filled troughs in the degraded, high-centered stage, would likely modify the results through reduced albedo, increased heat conduction and lower snow redistribution due to smaller elevation differences between the tiles. Results from model simulations, which take larger-scale hydrology into account, show increased soil ALT and earlier permafrost degradation when standing water is included (Langer et al., 2016; Nitzbon et al., 2018).*

*Nevertheless, adding further key processes to the two-tile system is likely to improve the simulation results. Here, we consider the representation of standing water as the most important process, followed by representation of vertically varying organic fractions and soil types, as well as dynamical vegetation. Most of these are already included in several large-scale LSMs (e.g. Lawrence et al., 2011; Reick et al., 2013).*

**Concerning the implementation in ESMs, it is clear that heterogeneity linked to excess ice is relevant only on a small part of the globe. In many other places, the most relevant heterogeneities are linked to vegetation, orography, or other factors. Can the authors think of a more general (globally relevant) tiling concept in which the tiling linked to excess ice could be integrated?**

This is a good point. We have added the following on this topic.

*Regardless of the choice of implementation, the method proposed here should be considered in the context of a larger effort to improve the representation of horizontal land processes ESMs. The land component of coupled atmosphere-land surface models is typically of considerable complexity in the vertical dimension, but includes little horizontal interaction and variation (see e.g. Clark et al., 2015). While representing heterogeneous excess ice is a relevant only in certain regions, we believe that a more flexible model structure with individual sub-grid soil columns that can exchange water and snow is a concept that deserves further investigation also in other regions.*

**In conclusion, I definitely think that this paper should be published if the points above and some specific points mentioned below are addressed. This should only require minor modifications.**

**Specific points:**

**P5 L28: FEXICE (and similar variable names in the text): In the figure, you use FEXICE (EXICE as an index), so please do so in the main text, too.**

Done!

**P6 L27: In the equation and in the text,  $K_{sat}$  is a constant. Call it  $K_{sat,0}$  for  $K_{sat}$  at the surface, to prevent confusion.**

Corrected. Thank you!

**P7 L10: "The lateral ground heat flux [. . .] between two grid cells with overlapping soil depth. . ." Cells or tiles? Probably tiles.**

This should be *tiles*, as you assumed. Corrected.

**P7 L17-18: Not clear why the elevated tile is used as a reference. In most models, there is no excess ice yet, so it might have been more appropriate to use the lower tile as a reference (especially because you do not use stagnant water at the surface anyway).**

By using the elevated tile as reference, we use Lee et al. (2014) as the starting point. This is now stated in the text. Although it is not common to include excess ice yet, this is more useful in terms of evaluating the effect of the different lateral fluxes.

*At both locations, a separate reference simulation (REF) is run with the same initial conditions as the elevated tile in the laterally coupled system (RIM or PPLAT), corresponding to the same model setup as employed in Lee et al. (2014), i.e. a 1D excess ice representation without lateral exchange.*

**By the way, it would have been nice, in the discussion, to spend a few lines on discussing how taking into account stagnant water could have changes the results. In my opinion, it could have very major impacts.**

See response to comment below (P.15L23).

**P7 L29: "This expands the soil thickness of the RIM with 1.5 m". Wouldn't "by 1.5 m" be better English?**

Yes. This has now been corrected.

**P8 L2: "we additionally add excess ice to the bottom soil layer (in both coupled tiles)": In the figure it looks like the 35 cm excess ice are added to the lowest layer only in the lower tile. Please clarify.**

Excess ice was added to both tiles, but with unequal amounts. This has now been clarified:

*To allow the RIM to sink below the elevation of the center, we add excess ice to the bottom soil layer, with the largest amount in CENTER, so that the total elevation difference is only 35 cm (Fig. A1). This is an approximate average value for observed rim heights at Samoylov.*

**P8 L14: "but still show continued": -> shows. In many places, there are wrong or missing s's (wrong plurals, wrong conjugation). Please go through the text carefully.**

Thank you for pointing this out. We have now corrected this and other similar errors.

**P8 L14: "making which makes"**

Corrected!

**P9 L2: I understand why you introduce figure 7 here before figures 5 and 6, but I think that the figure numbers should be in order of appearance in the text nevertheless.**

Agreed. We have now removed the reference to fig. 7 here so that the figure numbers agree with the order of appearance in the text.

**P9 L20: "simulation.." (only one point needed) Same line: "become is": ?**

Both corrected. Thank you!

**P10 L19: Why do you call the sensible heat flux HFX? Doesn't make much sense to me.**

This is the name of this variable in the NoahMP model, but we agree that this is not intuitive and have changed the name to the more commonly used *SH*.

**P11 L23: Replace whereas by while (I think)**

Changed. Thank you!

**P12 L16: scarcely -> barely?**

Changed. Thank you!

**P13 L26: "becoming in equilibrium": Are you sure that this is good English?**

We agree that this was not a good expression. This has now been rephrased:

*quickly reaching equilibrium*

**P14 L3: replace instantaneously by instantaneous (and does by do on the same line)**

Done.

**P14 L27: As said before, a sensitivity test showing the effect of the snow parameters would have been interesting. Or would that be too model-specific?**

See reply to comment above, including Fig. I.

**P15 L23: "Simulating instead surface water in low-centered polygons, or waterfilled troughs in the degraded, high-centered stage, would modify the results presented here." As said before, I'd like to see a discussion how this would modify the results (in your expert opinion)**

This has now been included, based on results from the Cryogrid model:

*Simulating surface water in low-centered polygons, or water-filled troughs in the degraded, high-centered stage, would likely modify the results through reduced albedo, increased heat conduction and lower snow redistribution due to smaller elevation differences between the tiles. Results from model simulations, which take larger-scale hydrology into account, show increased soil ALT and earlier permafrost degradation when standing water is included (Langer et al., 2016; Nitzbon et al., 2018).*

## Anonymous Referee #2

**In this paper, the authors take steps towards an ability to represent in a large-scale model the important lateral snow redistribution, water, and heat processes that impact the trajectory of permafrost thaw and related processes in different permafrost landscapes. The approach is parsimonious, which I like. The authors propose to represent these systems with just two ‘tiles’ (rim and center for polygonal tundra), rather than explicitly modeling the full complexity of the heterogeneous landscape. I like this approach as it does lend itself to potential inclusion across the pan-Arctic. A significant limitation is that the model is not explicitly modeling the formation of these permafrost landscape features. Instead, the goal is simply to be able to simulate the transition from a low-centered to a high-centered polygon. This is a reasonable first step and the authors acknowledge this limitation. Clearly, to have ‘full’ confidence in the model, one would want it to be able to simulate the full set of physical processes that drive both the formation and the decay of low-centered polygons. Nonetheless, this is a practical first step that is clearly an improvement over the current 1-tile assumption that cannot at all account for the real spatial heterogeneity of the system.**

As noted also in the reply to referee #1, we completely agree that simulating the formation of excess ice would be desirable, although we do not see this as feasible within the current study, both due to the long time scales, and the complexity and lack of well-developed parameterizations for the buildup processes.

**Overall, I enjoyed reading this paper and I find it suitable for publication with a few relatively minor revisions and clarifications.**

### Specific comments

**1. When the Noah-MP model is introduced, it would be good to explain why Noah-MP is being used instead of any other model. I believe that it is because of the lateral flow capabilities in WRF-hydro, but that capability isn’t introduced until section 2.2.4.**

We now include a short justification for the use of this model section 2.2, when the NoahMP model is first introduced.

*Furthermore, lateral subsurface water fluxes are already implemented in this model as part of the WRF-Hydro modelling system (see sec. 2.2.4). With some modifications it is therefore a suitable base model for studying the geophysical aspects of permafrost thaw, including the importance of lateral fluxes.*

**2. P. 8, line 2 typo: “only elevated only”**

Corrected. Thank you!

**3. I wonder if the “coupled” is the best way to reference the multiple tile simulations. Coupled can mean a lot of things in different contexts. Perhaps you could rename as Reference and Tiled or Single column and Two column or something else that is more descriptive.**

We agree that only referring to the two-tiled simulation as the “coupled” simulation is ambiguous. We have now carefully gone through the manuscript to make sure that whenever we refer to the “coupled” simulation, it is clear that we are referring to lateral coupling between tiles.

**4. Figure 5: Why is the ref simulation at depth so much warmer than either the RIM or**

## **CENTER simulation?**

We attribute this to the non-linear effect of snow. Maintaining an almost snow-free rim throughout the winter season increases the heat loss more on the RIM than it is reduced from the CENTER. The tiled system is therefore colder than the REF which receives the average snow accumulation.

**5. P.9, Line 16: “The simulated maximum snow depths in 2008 compares quite well with observations for both RIM (0.23 m compared to 0.16 m), and centers (0.39 m compared to 0.46) although the observations show considerable spread (see Nitzbon et al., 2018).” Statements like this are a bit misleading. Should make it clear that the simulated snow depths matching observations is probably mostly good fortune. You are using large-scale forcing from CRU-NCEP. It would be completely unsurprising if the snow depths didn’t match up with the observations at the local site when using large-scale forcing. It would be more appropriate to note that due to this good fortune, it is easier to make direct comparisons to observations.**

We agree that the raw CRU-NCEP data cannot be expected to reproduce local snow depths accurately, and the agreement is partly due to the scaling factor for precipitation. This is now noted in the text:

*This was partly achieved by applying a scaling factor for precipitation (Pscale) of 0.6 (Table 2).*

**6. P. 10, line 1: Similar to above, the discrepancy in temperature between model and obs is likely substantially a result of using the large-scale CRUNCEP data to force the model. You wouldn’t really expect the soil temperatures to match the observed site level soil temperatures in this circumstance.**

We again agree that one cannot expect to match soil temperatures exactly when forced with a large-scale reanalysis like CRU-NCEP. This is now pointed out in the discussion section.

*However, given the relatively coarse resolution of the forcing data, a certain disagreement must be expected*

**7. P. 13, line 4: Same again as above. The stability of the peat plateau is at least partly related to what you are getting from the large-scale forcing. You can’t go as far as to make the argument that you have to have certain couplings to maintain the peat plateau permafrost, which is what is implied. What you are finding, which is interesting and important, is just that soil conditions are colder on the peat plateau when snow and water coupling is included.**

We agree that permafrost could be maintained without these couplings in colder conditions. However, the snow and soil water conditions are recognized also by others as key factors for maintaining these marginal permafrost features in this region, which we now also include a reference for.

*This is in agreement with previous studies of palsas and peat plateaus in this region, pointing to low snow accumulation and dry peat during summer as the most important factors for their stability (see Seppälä, 2011).*

**8. The Discussion section brings up a lot of good points. One thing that isn’t clear in the discussion of how one could potentially employ this method at pan-arctic scale is the question of how one would specify the tile structure for each grid cell (is it a polygonal system or a peat plateau, something else, or a mixture of several permafrost landscapes within each large-scale grid cell). Along same lines, how would you know how to initialize the amount and depth of excess ice across the pan-Arctic domain? Based on the information provided in the paper, it seems like this took some trial and**

**error to get it 'right'.**

This is a good point. We have expanded the discussion with some more details on this:

*Ground ice data from Brown et al. (1998) could provide a starting point here, similar to the study by Lee et al. (2016). Assigning excess ground ice to the first soil layers below the simulated ALT has been a reasonable first-order choice for the two test sites, but this procedure is likely not adequate for areas with excess ice well below the current active layer, e.g. due to burial or melting of excess ground ice in the past (e.g. truncated ice wedges, Brown, 1967). Ultimately, new global data sets for ground ice depth, excess ice density and geometries of the two tiles must be compiled, for example building on approaches as in Hugelius et al, (2014) and Strauss et al., (2017).*

# Thaw processes in ice-rich permafrost landscapes represented with laterally coupled tiles in a Land Surface Model

Kjetil S. Aas<sup>1</sup>, Léo Martin<sup>1</sup>, Jan Nitzbon<sup>1,2,3</sup>, Moritz Langer<sup>2,3</sup>, Julia Boike<sup>2,3</sup>, Hanna Lee<sup>4</sup>, Terje K. Berntsen<sup>1</sup>, Sebastian Westermann<sup>1</sup>

<sup>1</sup> University of Oslo, Department of Geosciences, Sem Sælands vei 1, 0316 Oslo, Norway

<sup>2</sup> Alfred Wegener Institute, Helmholtz Centre for Polar and Marine Research, Telegrafenberg A45, 14473 Potsdam, Germany

<sup>3</sup> Humboldt University of Berlin, Geography Department, Unter den Linden 6, 10099 Berlin, Germany

<sup>4</sup> NORCE Norwegian Research Centre, Bjerknes Centre for Climate Research, Jahnebakken 5, 5007 Bergen, Norway

*Correspondence to:* Kjetil S. Aas (k.s.aas@geo.uio.no)

**Abstract.** Earth System Models (ESMs) are our primary tool for projecting future climate change, but their ability to represent small-scale land-surface processes ~~are is~~ currently limited ~~in their ability to represent small-scale land-surface processes~~. This is especially ~~the case~~ true for permafrost landscapes, ~~where in which~~ melting of excess ground ice and subsequent subsidence affect lateral processes which can substantially alter soil conditions and fluxes of heat, water and carbon to the atmosphere. Here we demonstrate how that dynamically changing microtopography and related lateral fluxes of snow, water and heat can be represented with through a tiling approach suitable for implementation in large-scale models, and investigate which of these lateral processes are important to reproduce observed landscape evolution. Combining existing methods for representing excess ground ice, snow redistribution and lateral water and energy fluxes in two coupled tiles, we show how that the same model approach can simulate known-observed degradation processes in two very different ~~kinds of~~ permafrost landscapes. Applied to polygonal tundra in the cold, continuous permafrost zone, we are able to simulate the transition from low-centered to high-centered polygons ~~which, and show how this~~ results in i) a more realistic representation of soil conditions through drying of elevated features and wetting of lowered features with related changes in energy fluxes, ii) up to 2 °C reduced average permafrost temperatures ~~at 13 m depth with up to 2 °C~~ in the current (2000-2009) climate, iii) delayed permafrost degradation in the future RCP4.5 scenario by several decades, and iv) more rapid degradation through snow and soil water feedback mechanisms once subsidence starts. Applied to ~~warm, peat plateaus in the~~ sporadic permafrost ~~features zone~~, this same two-tile system can represent an elevated peat plateau underlain by permafrost in a surrounding permafrost-free fen, and ~~how its~~ degradations in the future following a moderate warming scenario. These results ~~show demonstrate~~ the importance of representing lateral fluxes to realistically simulate both the current permafrost state and its degradation trajectories as the climate continues to warm. Implementing laterally coupled tiles in ESMs could improve the representation of a range of permafrost processes which is both of which are likely to ~~have important implications~~ impact for simulations of the simulated magnitude and timing of the permafrost carbon feedback.

## 1 Introduction

Permafrost landscapes represent an important, but complex component of the Earth's climate system. They currently cover approximately one quarter of the land area in the Northern Hemisphere (Zhang et al., 1999), and exert a major control on the local and regional hydrology and ecology. Moreover, it is estimated that approximately 1300 Pg carbon is stored in this region, which is considerably more than the current atmospheric carbon pool (Hugelius et al., 2014). If thawed and mobilized, this carbon could become a major source of greenhouse gas emissions (Schuur et al., 2008). ~~However~~ On the other hand, continued high-latitude warming and widespread permafrost thaw will likely ~~also~~ be associated with large-scale vegetation changes, which could act as an important carbon sink (Qian et al., 2010, McGuire et al. 2018). Understanding the future evolution of permafrost landscapes, and associated changes in the biogeochemical cycles, is therefore important for future estimates of climate change (Schuur et al., 2015).

Comprehensive Earth system models (ESMs) are our primary tools for estimating future climate change, including the magnitude and interplay between related-different climate feedbacks. ~~is the comprehensive Earth system models (ESMs).~~ Due to the possibly large impact of the permafrost-carbon feedback (PCF) on the climate system, permafrost processes have received much-significant attention in the development of these models during the last decade. Considerable improvements have been made by including freeze-thaw processes, multilayer soil carbon representation, increased soil depth and resolution, moss representation and multilayer snow schemes (Lawrence and Slater, 2005; Koven et al., 2013b; Chadburn et al., 2015; Burke et al., 2013). However, the representation of subgrid-scale permafrost processes remains a major limitation ~~remains in the lack of representation of subgrid-scale permafrost processes in of~~ these models (Lawrence et al., 2012; Beer, 2016). In particular, the ability to simulate changing microtopography resulting from melting of excess ground ice (thermokarst) is lacking. These processes are currently observed many places in the Arctic: ~~in~~ in polygonal tundra, Liljedahl et al. (2016) have documented how the transition of low- and flat-centered polygons (LCP and FCP) are transitioning into high-centered polygons (HCP), with large associated changes in local and regional hydrology. On the other hand, sporadic or isolated permafrost features like palsas and peat plateaus ~~can be~~ only maintained ~~only~~ through small-scale elevation differences and lateral fluxes of snow and water (Seppälä, 2011). Melting of excess ice in these features sets off a feedback mechanism through subsidence, enhanced snow accumulation, reduced winter heat loss and increased soil ice melt, which cannot be represented in a single large-scale grid cell. Accounting for these processes in ESMs is of particular importance since the regions with high amounts of excess ice ~~are largely coincide to a large degree also with regions/areas~~ with high amounts of soil carbon. Olefeldt et al. (2016) estimated that 20% of the northern permafrost region is covered by thermokarst landscapes, but suggested that as much as 50% of the soil organic carbon (SOC) in this region could be stored here.

Painter et al. (2013) described ~~the~~ the challenges with-of capturing the hydrologic response of degrading permafrost. ~~have been described by Painter et al. (2013), who~~ partitioned these processes into “subsurface thermal/hydrology, surface thermal processes, mechanical deformation and overland flow processes”. Some of these have been addressed in individual studies on local scales. For instance, polygonal tundra in Alaska has been simulated by Kumar et al. (2016) using a multiphase, 3D thermal hydrology model (PFLOPTRAN), by Grant et al. (2017) who included lateral fluxes of subsurface water as well as redistribution of snow and surface water, and by Bisht et al. (2018) who simulated a 104 m long transect with sub-meter

resolution including snow redistribution and lateral water and energy fluxes. In the warmer (discontinuous and sporadic) permafrost zones, Kurylyk et al. (2016) and Sjöberg et al. (2016) included groundwater flow and related heat advection in the simulation of peat plateaus in Canada and Sweden, respectively. Although capturing different aspects of lateral fluxes in ice-rich permafrost landscapes, these simulations have been performed with models ~~running-operating~~ on high-resolution grids which are not transferable to largescale Land Surface Models (LSMs). ~~Not-Furthermore, these studies~~ have ~~they-not~~ included ~~the-mechanical-deformation-microtopography-changes~~ ~~aspect-needed~~ to represent transient landscape ~~changes-evolution, or~~ ~~which-should-be~~ treated ~~this~~ in a unified way that can be applied to both continuous and discontinuous/sporadic permafrost features.

On the larger scale, Lee et al. (2014) included excess ground ice in a global LSM simulation which estimated land subsidence related to permafrost thaw and ground ice melt, but without including subgrid-scale variations and related lateral fluxes. Qui et al. (2018) included a separate subgrid tile in an LSM receiving surface runoff from the surrounding tiles to simulate peatlands with related carbon, moisture and energy fluxes. Gislås et al. (2016) and Aas et al. (2017) used subgrid tiles to represent heterogeneous snow accumulation, and showed how this influenced soil thermal regime and surface energy fluxes, respectively. Finally, Langer et al. (2016) employed a two-tile approach to simulate lateral heat exchange in polygonal tundra, ~~to-showing~~ that heat loss to surrounding land masses was ~~needed-required~~ to simulate stable thermokarst ~~ponds-lakes~~ in Northern Siberia.

In this study, Here we extend the two-tile approach of Langer et al. (2016) with lateral fluxes of snow and subsurface water flow, and combine this with the excess ice formulation of Lee et al. (2014). In this way, we can dynamically simulate changing microtopography ~~dynamically-together-which-impacts-with-the-effect-this-has-on~~ lateral fluxes of snow, water and heat. We thereby aim to for the first time simulate ~~dynamical-~~landscape changes due to excess ground ice melt, and related changes in lateral fluxes, in a framework suitable for implementation in ESMs. We apply this laterally coupled two-tile system to a polygonal tundra site in Northern Siberia and a peat plateau ~~location~~ in Northern Norway, and compare with results from a standard 1-D reference simulation. The two sites represent cold, continuous permafrost and warm, sporadic permafrost, respectively. Signs of permafrost degradation ~~can-are~~ currently be-found-observed at both locations, and small-scale heterogeneity in soil moisture and snow accumulation is a common feature for the two locations. Hence, they represent two very different climatic conditions for which -where current large-scale models fail to capture key small-scale processes that are important for the soil thermal regime. Aiming for a proof-of-concept rather than capturing the detailed properties at the test sites, By testing the model at these two locations we show to explore the capability of the simple two-tile system what extent the same simple model approach can to represent known-observed landscape changes and related water and energy fluxes, under very different permafrost conditions, and evaluate which of the lateral fluxes are important at the two locations. Capturing the detailed properties at the specific test sites is not the objective of this study, but rather to show how the general behavior observed in these landscapes can be represented in a way suited for large-scale models.

## 2 Methods

### 2.1 Site descriptions

The model is applied to the two permafrost locations shown in Fig. 1. Samoylov Island in northern Siberia represents a polygonal tundra location in cold, continuous permafrost, ~~whereas while the~~ peat plateaus in Suossjavri, northern Norway, represents warm, sporadic permafrost. Both locations are, however, examples of carbon- and ice-rich permafrost landscapes ~~where in which~~ small-scale lateral fluxes ~~are important for representing the of water, heat and snow are known to occur physical state of permafrost.~~

#### 2.1.1 Samoylov Island, Northern Siberia

Samoylov Island (72°22'N, 126°28'E) is located in the southeast corner of the Lena River delta. The size of the entire Delta, including more than 1500 islands and about 60 000 lakes, is about 25 000 km<sup>2</sup> (Fedorova et al., 2015), and ~~the area is~~ underlain by continuous, cold permafrost. The island of Samoylov, located in the southern part of the delta, mainly consists of polygonal tundra ~~surrounding with~~ a number of ponds and lakes (Fig. 1b; Boike et al., 2013, 2018). All degradation stages described by Liljedahl et al. (2016) can be found here, from non-degraded low-centered polygons to high-centered polygons with connected troughs (see Nitzbon et al., 2018). Between 1997 and 2017, the mean annual air temperature at the island was approximately -12.3 °C, with an annual liquid precipitation of 169 mm and mean end-of-winter snow depth of 0.3 m (Boike et al., 2018). ~~At the The~~ depth of zero annual amplitude ~~is at~~ (20.8 m), and ~~the permafrost~~ has warmed from - 9.1 °C in 2006 to - 7.7 °C in 2017. Numerous studies have been conducted on the island, including ~~studies investigations~~ of water and surface energy balance (Boike et al., 2008, Langer et al., 2011a, b) and carbon cycling (Knoblauch et al., 2018; Knoblauch et al., 2015). As a well-studied site with available meteorological, soil physical, and hydrological measurements (Boike et al., 2018), it has also been used as test site for various permafrost modelling studies, including ESM validation and development (Chadburn et al., 2015; Chadburn et al., 2017; Ekici et al., 2014; Ekici et al., 2015).

#### 2.1.2 Suossjavri, Northern Norway

Suossjavri (69°23'N, 24°15'E) is situated in the central part of Finnmark county in northern Norway. It is part of the sporadic permafrost zone in northern Fennoscandia (Fig. 1), where permafrost outside mountain regions is confined to palsas and peat plateaus in mires. The site has an elevation of approximately 335 m asl and covers ~~over e.a. about~~ 23 ha. It is bordered by the Isjoka River on the South and the Suossjavri Lake on the East and North and consists of ~~metric to decametric~~ palsas and peat plateaus that rises ~~20 cm up~~ to 2 m above the ~~seven~~ surrounding wet mires. ~~These permafrost bearing morphologies These permafrost features are degrading strongly are currently degrading, and have~~ ~~ing~~ lost approximately 30 % of their area in the last six decades (Borge et al., 2017). Largest degradation rates are seen for the smaller palsas and peat plateaus, which have lost almost half ~~of~~ their areas in this period, compared to only 15% ~~degradation aerial loss~~ of the ~~four largest~~ peat plateaus.

The mean annual air temperature in the region ~~is usually range comprised between~~  $-2^{\circ}\text{C}$  ~~and to~~  $-4^{\circ}\text{C}$ , with a summer mean value of  $10^{\circ}\text{C}$  (JJA) and winter value of  $-15^{\circ}\text{C}$  (DJF, Aune, 1993, for the 1961-1990 period). The mean annual precipitation is below 400 mm according to the nearest measurement station (Borge et al., 2017). Mean annual ground surface temperatures (MAGST) have been measured with iButton® temperature loggers at 25 locations ~~across one of the mires~~ since September 2015, ~~along in conjunction~~ with end-of-summer thaw depths and end-of-winter snow depths at the same points. These show snow depths on the ~~interior~~ peat plateaus mostly between ~~zero-0~~ and 40 cm, ~~an ALT~~ active layer thickness (ALT) between 40 cm and 70 cm, and  $1^{\circ}\text{C}$  to  $2^{\circ}\text{C}$  colder MAGST ~~than compared to~~ the surrounding ~~mires~~ wet mire areas.

## 2.2 The NoahMP land surface model

~~Our~~ The modeling study is performed with the NoahMP LSM version 3.9, with a number of modifications described below. In its default configuration the NoahMP model (Niu et al., 2011) simulates soil temperature and frozen and liquid water in four soil layers down to a depth of 2 m. It includes up to three snow layers with representation of liquid water retention and refreezing, as well as a separate canopy layer. Compared to the original Noah code, NoahMP is an augmented version that includes multiple alternative model representations for key processes, including parameterizations of supercooled liquid water and frozen ground hydraulic conductivity (see details in Niu et al., 2011). It is substantially less complex and computationally expensive than LSMs used in current state-of-the-art ESMs, ~~disregarding-lacking~~ for instance ~~representations of~~ biogeochemical processes and dynamical vegetation. However, in its basic treatment of soil thermal and hydrological processes, it is comparable to, and includes some of the same parameterizations as, the Community Land Model (CLM; Lawrence et al., 2011). ~~Furthermore, lateral subsurface water fluxes are already implemented in this model as part of the WRF-Hydro modelling system (see sec. 2.2.4). With some modifications it is therefore a suitable base model for studying the geophysical aspects of permafrost thaw, including the importance of lateral fluxes.~~ In the following, we will describe the modifications and augmentations to the NoahMP model for our simulations.

### 2.2.1 Soil resolution, excess ice and soil organic fraction

To better represent permafrost processes, the number of soil layers was increased from the default four to 37, with the total soil depth increased from 2 m to 7 m or 14 m, plus excess ice thickness (Fig. A1). These soil depths were chosen to approximately include the zero annual amplitude depth at Suossjvari and Samoylov, respectively, but still be shallow enough to avoid long spin-up times, as the emphasis ~~here-of this work~~ is on ~~the~~ near-surface processes rather than ~~the~~ deep soil conditions.

Secondly, we added soil organic fraction as an additional (fixed) input variable. Following Lawrence and Slater (2008), soil thermal and hydraulic properties were calculated assuming a linear weight between organic and the (original) mineral fractions. This ~~allowed us to facilitated~~ simulating organic rich soils like peat ~~whose, which has~~ properties ~~are very~~ different ~~than from~~ the default soil types available in NoahMP.

Following Lee et al. (2014), we included excess ice within the existing layers ~~in-of~~ the model, so that the layer thicknesses and properties of the layers change throughout the simulation as the excess ice melt. Excess ice is initialized as a

certain fraction ( $F_{exice}$ ), within a certain depth region in each soil column (see Fig. 3 and A1). Because excess ice is incorporated as an initial condition, it only melts and does not grow. The water from melting excess ice is added to the soil column in the layer where it melts, or the nearest unsaturated layer above if this layer is saturated.

### 2.2.2 Implementation of interacting tiles

Sub-grid tiles have been implemented in the original Noah version as part of the Weather Research and Forecasting model (WRF) to represent a mosaic of land cover types (Li et al., 2013). This tiling included soil columns simulated independently for each tile, but without any interaction between the tiles during the simulation. Here we build upon this methodology to explicitly simulate individual land units within a grid cell, but include also lateral fluxes as described below. In the following general description of the interactive tiles, we will refer to these as tile 1 and 2, but later refer to them as RIM and CENTER for the polygonal tundra and PPLAT and MIRE for the peat plateau setting (Fig. 2).

### 2.2.3 Snow redistribution between interactive tiles

To represent the effect of snow redistribution by wind, we scale the amount of snow received in tile 1 and 2 based on the difference in elevation at the top of the snow/soil column. Similar to Aas et al. (2017), this is done with a scaling factor, so that the accumulation of snow in tile  $i$  is calculated according to the grid-cell mean snowfall  $S$ , times the scaling factor  $f_i$  ( $S_i = f_i * S$ ).

The scaling factor is calculated as follows: ~~if~~ For snow depths below a minimum snow value ( $HS_{min}$ ), no redistribution takes place, ~~i.e.~~

$$f_i = 1.0, \text{ for } HS_i < HS_{min}, \quad (1)$$

Once the tile with the highest elevation reaches the minimum snow value, the scaling factor is calculated so that no new snow accumulates on this tile before the total snow and soil elevation ( $z_i$ ) ~~is-are~~ within 5 cm of each other:

$$f_{1,2} = \begin{cases} 1.0, & \text{for } |z_1 - z_2| < 0.05m \\ 0.0, & \text{for } (z_{1,2} - z_{2,1}) \geq 0.05m \\ 1.0 + \frac{A_{2,1}}{A_{1,2}}, & \text{for } (z_{2,1} - z_{1,2}) \geq 0.05m \end{cases}, \quad (2)$$

where  $A$  refers to the area of the tile, and the subscript refers to the tile number (1 or 2).

### 2.2.4 Lateral subsurface water flux between interactive tiles

Lateral water flux is calculated similar to subsurface flow in WRF-hydro (Gochis et al., 2015), with a few modifications relevant for permafrost conditions. The flow rate [ $m^3 s^{-1}$ ] from ~~a~~ one tile to another can be calculated as

$$q = \begin{cases} -T \tan(\beta) L, & \text{for } \beta < 0 \\ 0, & \text{for } \beta \geq 0 \end{cases} \quad (3)$$

where  $T$  is the transmissivity,  $L$  is the contact length and  $\beta$  is the water table slope between the tiles.  $T$  is given by

$$T = \begin{cases} \frac{K_{sat,0} Z_B}{n} \left(1 - \frac{z_{wt}}{Z_B}\right)^n, & \text{for } z_{wt} \leq Z_B \\ 0, & \text{for } z_{wt} > Z_B \end{cases} \quad (4)$$

Here  $z_{wt}$  is the water table depth,  $Z_B$  is the total soil depth,  $K_{sat,0}$  is the saturated hydraulic conductivity [at the surface](#) and  $n$  is a tunable local power law exponent determining the decay rate of  $K_{sat}$  with depth.

Here we set  $n = 1$ , and use the depth to the minimum (highest) frost table depth ( $z_{frzmin}$ ) instead of the full soil depth  $Z_B$ . Inserting  $\tan(\beta) = \frac{z_{wt1,2} - z_{wt2,1}}{D}$ , where  $D$  is the distance parameter, the flow rate can then be calculated as:

$$q_{1,2} = \begin{cases} -WK_{sat} \frac{z_{wt1,2} - z_{wt2,1}}{D} (z_{frzmin} - z_{wtmin}), & \text{for } z_{frzmin} \geq z_{wtmin} \\ 0, & \text{for } z_{frzmin} < z_{wtmin} \end{cases} \quad (5)$$

Here we set the frost table to the top of the first layer (from the top) with more than 1 % volumetric soil ice (including excess ice). The water table depth is taken as the depth to the top of the first saturated soil layer.

### 2.2.1.5 Lateral ~~ground~~ heat flux between interactive tiles

The lateral ground heat flux [ $\text{W m}^{-2}$ ] between two [grid-cell tiles](#) with overlapping soil depth of  $\Delta Z$  can be calculated as (see Langer et al., 2016):

$$q_{S1,2} = \frac{L}{A_{1,2}} k_s \frac{T_{2,1} - T_{1,2}}{D} \Delta Z, \quad (6)$$

where  $k_s$  is the thermal conductivity. This is calculated individually for each partially overlapping soil layer.

## 2.3 Model setup and forcing

The model setup is shown in Fig. 3 and Table 1 and 2 and described separately for the two locations in the following, together with the forcing data for the corresponding locations. In both cases, a model timestep of 15 min is applied, with zero flux as the lower thermal boundary condition. To represent larger-scale landscapes with a small number of tiles, we exploit the concept of self-similarity (i.e. translational symmetry). At both locations, a separate reference simulation (REF) is run with the same initial conditions as the elevated tile in the [laterally](#) coupled system (RIM or PPLAT), [corresponding to the same model setup as employed in ~~By using this as the reference, we use excess ice study by Lee et al. \(2014\), i.e. a 1D as the starting point~~ excess ice representation without lateral exchange](#). The other (initially lower) tile in the [laterally](#) coupled simulation is referred to as CENTER and MIRE for the tundra and mire locations, respectively.

### 2.3.1 Polygonal tundra on Samoylov Island, Northern Siberia

The polygonal landscape at Samoylov Island is ~~here~~ represented ~~with-by~~ two tiles that represent center ~~regions~~ and rim ~~regions~~ [areas](#), respectively. These are in reality of different sizes and shapes (Fig. 1), but can to a first approximation be considered a self-repeating pattern, as also described by Nitzbon et al. (2018). Due to symmetry, a larger region can then be

represented as a single feature with a representative geometry, ~~where neglecting~~ the interaction between ~~the~~ different polygons ~~can be ignored~~. For simplicity, we here simulate a representative polygon as a circular feature with center and rim of equal area, and a total diameter of 10 m. Assuming ~~instead~~ hexagons ~~instead of circles~~, like Nitzbon et al. (2018), would only require minor modifications to the parameters shown in Fig. 3, particularly the distance parameter and the interaction length.

To represent an ice wedge occupying the majority of the soil volume, we initialize the RIM ~~tile~~ with an excess ice fraction of two thirds between the simulated ALT at 55 cm and 2.8 m below the surface. ~~This, which~~ expands the soil thickness of the RIM ~~with by~~ 1.5 m. To allow the RIM to ~~degradesink~~ below the elevation of the center, we ~~additionally~~ add excess ice to the bottom soil layer, ~~with the largest amount in CENTER, (in both coupled tiles)~~ so that the ~~top of RIM is only elevated~~ ~~total elevation difference is~~ only 35 cm ~~relative to CENTER~~ (Fig. A1), ~~which~~ This is an approximate ~~middle-average~~ value for observed rim heights at Samoylov. The model is ~~initiated~~ initialized with a soil temperature of -9 °C and fully saturated and frozen soil throughout the column. ~~This~~ While this is substantially colder than the equilibrium temperature reached by the model. ~~However, the soil temperatures in the lowest cell (lower boundary at ca. 16m, i.e. 14 m plus 2.15-2.5 m excess ice) reach an equilibrium within the first decade of the simulation (mean increase of 0.3 °C yr<sup>-1</sup>), with total soil column of about 16 m (14 m plus 2.15-2.5 m excess ice including bottom ice, less than the observed depth of zero annual amplitude), the deep soil temperatures are spun up within the first decade of the simulation (mean increment of 0.3 °C yr<sup>-1</sup>), after which the annual increments changes~~ vary between positive and negative values.

As model forcing for the Samoylov Island simulation, we used the same model input as Westermann et al. (2016). This is based on the CRU-NCEP data for the historical period (1901-2015; Viovy, 2018). For the future part of the simulation, this dataset uses model output from the CCSM4 climate model following the mitigation scenario RCP4.5, to calculate monthly climate anomalies for temperature, humidity, pressure and wind, and scaling factors for precipitation and radiation. These are added or multiplied to the high-frequency data from 1996-2005 from the historical (CRU-NCEP) data, ~~This methodology follows~~ Koven et al. (2015). The RCP4.5 scenario was chosen as it represents a strong mitigation ~~scenario effort, and is hence an optimistic scenario,~~ but still shows continued warming in the Arctic throughout the 21<sup>st</sup> century ~~making~~ which makes understanding permafrost processes highly relevant.

~~Detailed measurements of snow accumulation from 8 low-centered polygons from 2008 showed average snow depths of 17 cm on the rims, and 46 cm in the centers, with a total average SWE of 65 mm (Boike et al., 2013). As the model accumulated too much snow compared to these observations due to a bias in the precipitation forcing (Westermann et al., 2016), we scaled the precipitation with a constant factor ( $P_{scale}$ ) of 0.6 throughout the simulation in order to simulate realistic SWE and snow depths. One modification was made to this dataset in the current study, as it was observed that the model accumulated too much snow compared to observations. Detailed measurements of snow accumulation from 8 low-centered polygons from 2008 showed average snow depths of 17 cm on the rims, and 46 cm in the centers, with a total average SWE of 65 mm (Boike et al., 2013). In order to simulate similar SWE and snow depths, we scaled the precipitation with a constant factor ( $P_{scale}$ ) of 0.6 throughout the simulation. The resulting mean annual temperature and precipitation for the whole period is seen in Fig. 4a.~~

### 2.3.2 Peat plateaus in Suossjavri, Northern Norway

Similar to the polygonal tundra, the peatland of Suossjavri is represented with two interacting land units. In this case we represent a single, circular peat plateau with a diameter of 10 m, corresponding to the smaller features observed ~~at-in~~ the study area. This is placed in a significantly larger (100 m x 100 m) surrounding mire, so that the effect of the coupling ~~is-mainly~~ affectson the elevated tile. The areas of both the mire and the peat plateau can be increased to represent larger features (see Sect. 4.2), and more complex geometries can be represented by applying appropriate distance and contact length parameters. As the mire does not contain permafrost, only the peat plateau tile (PPLAT) was initiated with excess ice (Fig. A1b), starting 75 cm below the surface, ~~and~~ with a total excess ice thickness of 75 cm distributed down to 3.75 m below ground. Both tiles were started from fully saturated conditions and 0 °C soil temperatures. The soil water was initially unfrozen in all soil layers, except for the ones containing excess ice, where-in which soil (pore) water was initially frozen.

Forcing data for this location ~~was-were~~ generated in a similar way as the data used at Samoylov Island. CRU-NCEP data from nearest grid point ~~was-were~~ used for the historical ~~alal~~ part, whereasile anomalies for the future (starting in year 2010) were taken from an CCSM4 simulation following the RCP4.5 scenario and added/multiplied to the reference period 1996-2005. ~~The resulting mean annual temperature and precipitation for the whole period is seen in Fig. 7a.~~

## 3. Results

In the following, we ~~will look at the~~ outline the model results ~~of the two laterally coupled tiles compared to the uncoupled reference tile, beginning with for~~ the polygonal tundra site in Northern Siberia (~~section Sect. 3.1~~) ~~and, before looking at the~~ peat plateau location in Northern Norway (~~section Sect. 3.2~~).

### 3.1 Samoylov Island, Northern Siberia

During the ~~course of our~~ simulation period, Samoylov island experiences a strong increase in annual mean air temperature and a modest increase in precipitation (Fig. 4a). Mean air temperatures rise-increase from approximately -14 °C in the early 20<sup>th</sup> century to as-high-asabout -8 °C towards the end of the 21<sup>st</sup> century ~~with the~~ (RCP4.5 scenario), with most of the warming happening-occurring during in the 21<sup>st</sup> century.

Both the reference and the laterally coupled simulations show stable permafrost with ALT between 0.45 m and 0.65 m during the historical period of the simulation (until 2010). This is in good agreement with observations, showing mean ALT close to 0.5 m (Boike et al., 2013; 2018). For snow depth and near surface soil moisture conditions, the laterally coupled simulations show clear differences from REF (Fig. 4 b and c); and mimic more-closely-mimies the observed conditions more closely (see Boike et al., 2013; 2018 and Nitzbon et al., 2018). The simulated maximum snow depths in 2008 compares quite well with observations for both RIM (0.23 m compared to 0.16 m), and centers (0.39 m compared to 0.46), although the observations show a considerable spread (see Nitzbon et al., 2018). This was partly achieved, This agreement is partly due to by applying the scaling factor for precipitation applied to this site ( $P_{scale}$ ) of 0.6 (Table 2). In agreement with observations (see Chadburn et al., 2017 and Nitzbon et al. 2018), the model displays ~~D~~ dry near-surface soil conditions in the RIM ~~tile~~; and

mostly saturated conditions in the -CENTER tile, is also what is observed in this landscape (see Chadburn et al., 2017 and Nitzbon et al. 2018), ~~a distinction~~ which cannot be represented in the REF simulation. With increasing the rising air temperatures in the 21<sup>st</sup> century, the ALT deepens and surface subsidence occurs in REF, reaching 35 cm the difference between the laterally coupled tiles and REF become is also seen in that ALT deepens and subsidence begins in REF. Aarround 2030 the subsidence in REF has reached 35 cm, and more than 1 m by the end of the century the subsidence is more than 1 m, with the ALT still growing. In the coupled two-tile simulation, RIM remains relatively stable and elevated above the center until around 2070, almost four decades later than REF. RIM subsequently subsides due to excess ice melt, eventually sinking below CENTER, which marks the transition from LCP to HCP. Towards the end of the simulation RIM appears to stabilize with a subsidence of 80cm and an ALT of less than 1 m, ~~which is also~~ in contrast to the uncoupled single-tile REF.

CENTER experiences ALT deepening in the 21<sup>st</sup> century, which reaches a maximum around 2070. ~~This-The~~ deepening of the active layer follows the rapid increase in forcing temperature, and lasts until RIM has subsided below CENTER. After this point the elevated RIM tile has turned into a trough, and the top layers in CENTER starts to drain, resulting in shallower ALT. This marks the transition from a low centered to a high centered polygon.

*Soil temperatures:* The annual cycle of the soil temperature is shown in Fig. 5. In current climate (left column), the elevated rim shows annual temperature variations in the active layer of more than 20 °C, in agreement with observations (Boike et al., 2018). At depth, the soil temperatures are higher than observed, with values around about -3 °C in REF and -5 °C in the laterally coupled simulations, compared to -8.6 °C at 10.7 m depth observed during the second half of this decade (Boike et al., 2013). Here it is worth noticing, however, that ~~these-these~~ temperatures are rising, and have increased more than 1 °C during the last decade (Boike et al., 2018).

Again, clear differences can be seen between REF and the laterally coupled tile system. In the current climate (left column), REF and CENTER shows a very similar annual cycle, whereas the amplitude of the temperature cycle is much larger in RIM. In the active layer, the difference is almost exclusively observed during winter, when the effect of shallower snow depth is decreasing the winter insulation in RIM. Deeper ~~into-in~~ the soil column the differences in soil temperature become less pronounced between the two coupled tiles (RIM and CENTER) ~~show much more similar temperatures~~, as heat exchange between the ~~two~~ tiles becomes more important. In the deep soil (Fig. 5c) the temperature is ~~therefore~~ similar (within 0.5 °C), but around two degrees colder than in REF. ~~Similar results are seen for the~~ At the end of the century (Fig. 5b), ~~except with opposite characteristics for the two coupled tiles~~ the situation has reversed and- ~~The~~ now elevated, dry CENTER with low snow accumulation has become the tile with the large annual amplitude in the top soil feature cold winter temperatures, whereas RIM largely follows REF. Deeper ~~into~~ the soil, ~~we again see both~~ the two coupled tiles are being again colder than REF, although the difference is smaller than in the beginning of the century (Fig. 5d). Comparing the temperatures at 2 m depth from the surface in REF and the area-weighted mean of the two coupled tiles (here mean of RIM and CENTER), we find the coupled simulation on average 2.1 °C colder than REF during the 20<sup>th</sup> century. This difference decreases to almost zero during the transition from LCP to HCP, before the coupled simulation becomes 1.4 °C colder ~~1.4 °C~~ during the final two decades of the simulation.

*Summer surface energy fluxes:* A clear difference between the tiles is ~~also~~ seen in the summer surface energy fluxes (Fig. 6). As expected, the dry RIM shows larger sensible (~~SHHF~~~~X~~) and lower latent (LH) heat fluxes than REF before degradation, whereas the wet CENTER shows the opposite (Fig. 6 a). This is reversed ~~at~~~~in~~ the degraded state when CENTER is dry and the trough (subsidised RIM tile) is wet. Interestingly, the landscape aggregated values (here the mean of RIM and CENTER) is only a few  $\text{W m}^{-2}$  different from the reference for these two fluxes both before and after degradation (Fig. 6a, b). We note, however, that this depends on drainage conditions. Here only surface water (infiltration excess) is removed as runoff, whereas advanced degradation ~~in~~~~of~~ this kind of polygons is often associated with drainage also of the troughs (Liljedahl et al., 2016). This effect is not included here, but is simulated and discussed by Nitzbon et al. (2018), and would likely ~~move~~ ~~increase~~ the Bowen ratio of laterally coupled tiles ~~towards higher Bowen ratios~~~~at~~~~in~~ the degraded stage compared to both REF and the non-degraded stage. It is also likely that the difference between the reference simulation and the aggregated values would be larger with a different areal fraction of RIM compared to CENTER.

The ground heat flux (GRDFLX) is lower during both time periods for the mean of the two coupled tiles than the REF, due to a substantially reduced flux in the dry, elevated tile (first RIM, then CENTER). This points to the effect of dry peat insulating the soil, and suggests that the lower temperatures in the laterally coupled system could be a result of both increased summer insulation as well as the reduced winter insulation mentioned above.

Qualitatively, our simulation captures the observed difference between the RIM and CENTER reported by Langer et al. (2011b), although the simulation seems shifted towards higher sensible heat fluxes and lower latent heat fluxes. This again might be related to too low water holding capacity in our simulations, as well as the lack of surface water on top of the low-centered polygon.

### 3.2 Suossjavri, Northern Norway

Figure 7 shows the soil moisture, surface elevation, ALT and snow depth at the mire location in the sporadic permafrost zone in Northern Norway. ~~In~~~~Here~~ REF, permafrost starts to degrade at the beginning of the simulations~~is unable to maintain permafrost, and, with the~~ excess ice ~~is~~ rapidly disappearing ~~during~~~~over~~ the first 3-4 decades of the simulation. After this point, REF ~~aets~~~~has turned into as~~ a mostly saturated wetland with maximum snow depths around 1 m. The corresponding tile in the laterally coupled system (PPLAT) experiences low maximum snow depths and dry surface conditions (Fig. 7c), which results in a thermally stable peat plateau throughout the 20<sup>th</sup> century. Compared to observations at this location (see Sec. 2.1.2), the PPLAT shows asomewhat somewhat larger ALT (0.75 - 0.9 m) in the historical period. The initial excess ice does not start to melt until around 2030, ~~which is~~ when both air temperatures and precipitation starts to ~~increas~~~~ing~~ rapidly. Accelerating ALT deepening in conjunction with surface subsidence due to excess ice melt is seen after 2050. ~~At this point, when~~ the mean air temperature has stabilized at about -1 °C and precipitation around 650 mm. ~~However, t~~ ~~This~~ ~~he~~ acceleration of the ALT deepening process appears to be driven by feedbacks in the system: ~~First, we have the melt-subsidence-snow feedback. As~~ the ATL deepens and excess ice melts, the peat plateau subsides, leading to more snow remaining in this tile and smaller heat loss during winter, which again enhances summer melt. ~~Next~~Furthermore, the subsidence also results in a thinner layer of dry peat as the water table is largely controlled by the surrounding wet mire, which lowers the insulation

during summer. Combined with the direct effect of water from the excess ice melt increasing the soil moisture in PPLAT, this leads to a melt-subsidence-soil moisture feedback, in addition to the melt-subsidence-snow feedback. The surrounding MIRE is largely unaffected of by the presence and disappearance of the elevated peat plateau as it is here simulated assumed to be about two orders of magnitude larger. Hence, REF and MIRE develop very similarly after the initial excess ice in REF has melted.

*Soil temperatures:* The soil temperatures in the laterally coupled tiles differs substantially in the present, non-degraded state (Fig. 8 a, c). Whereas-While REF and MIRE have nearly identical annual temperature cycles near the surface, PPLAT deviates on-in several points. First of all, the elevated PPLAT shows cold winter soil temperatures (as low as -7.6 °C in January), compared to a constant, zero-degree temperature in MIRE and REF. Furthermore, PPLAT responds quicker to the onset of both summer and winter, with both MIRE and REF shifted somewhat to warmer temperatures in late summer and colder temperatures during spring. One key factor controlling these differences is the low snow accumulation in PPLAT, which lead to both increased annual temperature cycle near the surface, and an earlier onset of spring due to less energy going to snow melt. Another factor is the higher soil moisture in REF and MIRE (both mostly saturated), which due to the high heat capacity of water will delays the soil response to changing atmospheric temperatures.

Below the depth of zero annual amplitude, PPLAT sees-displays warm permafrost conditions at zero-0 °C, whereas the MIRE and REF is feature temperatures close to 3 °C. Here there is a slight difference between the REF and MIRE, with the former being simulations are about a quarter of a degree 0.25 °C colder than MIRE, due to the memory at which is most likely a legacy -this depth of excess ice from ice melting earlier in the simulation (Fig. 7).

After degradation (Fig. 8 b, d), the differences between the three realization near the surface is are marginal between all three realization near the surface. At this point, there is no elevation difference, and hence no so that differences in snow accumulation or and other surface forcing at the parameters vanish surface. The dSome differences remain in is then confined to the lower deeper soil layers, where the PPLAT tile is still continues to warming after the ice melt.

*Summer surface energy fluxes:* The different snow and soil conditions between the MIRE and PPLAT are also clearly visible in the summer surface energy fluxes (Fig. 9). In the present, undegraded state, the PPLAT tile shows almost opposite SH HFX and LH fluxes compared to both MIRE and REF, which again are practically identical. Whereas-While the MIRE and REF both shows three to four times larger LH than SH HFX, the opposite is the case for the dry, elevated PPLAT. At this location, unlike the polygonal tundra site, the average over the two coupled tiles would differ substantially from REF. As the MIRE is two orders of magnitude larger than PPLAT in the present model setup, the aggregated fluxes is are only be marginally different than what a from the single MIRE tile (similar to REF). However, observed peat plateaus can occupy a large area of the landscape (as also seen from Fig. 1b), and configurations with representing MIRE and larger PPLAT area of more equal size will would likely result in larger differences in the aggregated fluxes.

For the ground heat flux (GRDFLX) the differences are smaller, but still substantial. The elevated PPLAT receives on average less energy from the surface during summer compared to both RIM and MIRE. With colder temperatures at depth in this tile, this points to the insulating effect of dry peat as being a contributor to sustaining permafrost, in addition to the above-mentioned winter effect from due to shallower snow depths. In the degraded phase, the difference between all three

realizations have nearly vanished, as the PPLAT is no longer elevated from the MIRE. Here only a slightly larger GRDFLX (~~scarcely barely~~ visible) shows that temperatures ~~below in deeper layers are still adjusting from after the ice melted~~ have not yet reached an equilibrium.

#### 4. Sensitivity studies

To further investigate the importance of the different processes in the laterally coupled system, we perform two sets of sensitivity studies. First, we look at the effect of ~~selectively turning on anactivating off the~~ different lateral fluxes at both locations, before ~~looking further investigating at~~ the effect of the distance parameter (D) for the simulation of the peat plateau location.

##### 4.1 Snow, water and heat coupling

Figure 10 shows the surface elevation in the initially elevated tiles (RIM/PPLAT) at both locations for different combinations of lateral fluxes. Here, the tick blue ~~and red lines line~~ represents the reference simulation (similar to REF), ~~whereas the simulation with all lateral fluxes activated are included and the fully coupled~~ (similar to RIM/PPLAT) is shown with a thick red line and realizations in section 3, respectively. (in the following referred to as “fully coupled”).

For the polygonal tundra site (Fig. 10a) the snow effect alone (thin red) gives similar results as the fully coupled simulation during most of the time period. The difference is clear only towards the end, when the snow-only experiment continues to melt and subside with a trough approaching 1 m depth (corresponding to 1.35 m subsidence), ~~whereas while~~ the fully coupled system stabilizes with a 45 cm trough. ~~Individually a~~ Adding lateral water (yellow) or heat (purple) fluxes has opposite effects, decreasing and increasing the melting process, respectively. The snow +plus water coupling (green) results in an almost stable rim throughout the simulation, subsiding only about 10 cm before the end of the 21<sup>st</sup> century, whereas the snow +plus heat coupling (thin blue) results in about 10 years earlier subsidence than the fully coupled realization, but eventually stabilizing at almost the same depth.

At the peat plateau location in Northern Norway, the combined effect of snow and water coupling is needed to simulate a stable peat plateau throughout the 20<sup>th</sup> century ~~with the forcing used here~~ (Fig 10b). Only the fully coupled (tick red) and the snow +plus water coupling (green) can represent stable permafrost, whereas all other simulations ~~see display~~ degradation starting within the first decades of the 20<sup>th</sup> century and ground ice disappearing entirely before 1970. This is in agreement with previous studies of palsas and peat plateaus in this region, pointing to low snow accumulation and dry peat during summer as the most important factors for their stability (see Seppälä, 2011). Adding the lateral heat flux to the reference setup (purple) has little effect. However, in combination with the snow and water coupling, the heat flux ~~is speeding speeds~~ up the melt, so that the peat plateau disappears two decades earlier than ~~without the heat coupling in the simulations without lateral heat fluxes~~.

~~Seen In conclusion together~~, it appears that all three lateral fluxes are important at both locations. Compared only to the reference simulation, the effect of snow redistribution is largest, followed by the effect of coupling through water fluxes

coupling, whereas the effect of the lateral heat flux alone is marginal. However, both snow and water coupling act to cool the elevated tile compared to the CENTER/MIRE, as seen by the delayed subsidence. Hence, an increased thermal gradient between the different tiles is produced/generated that which increases the effect of the lateral heat flux, reducing the. The result is that the stabilizing effect of snow and water fluxes are reduced, and speeding up degradation, speeded up. The relative effect of the different processes is therefore complex, and must be seen in combination with the other fluxes.

The influence of the different lateral fluxes is to some degree sensitive to process implementation and the key model parameters and how it is implemented. This is especially the case for snow redistribution, which in our simulations was found to be the most important coupled-lateral process. Here, we redistribute all solid precipitation from the tile with the highest surface elevation (soil + snow), once a minimum snow depth is reached ( $H_{s_{min}}$ ). Increasing (decreasing) this limit will decrease (increase) the effect of snow redistribution in the simulation. An additional set of sensitivity simulations with different values of  $H_{s_{min}}$  ranging from 0.0 to 0.15 m (not shown) revealed that the landscape evolution at the polygonal site was relatively insensitive to this value, with the transition from LCP to HCP shifting by less than two decades between the minimum and maximum value. A larger sensitivity was seen for the peat plateau site, for which the lowest values of  $H_{s_{min}}$  resulted in stable permafrost throughout the 21<sup>st</sup> century. Similarly, the thermal and hydraulic conductivity of the soil will determine the effect of the heat and water fluxes, respectively. However, the effect of lateral heat flux was only important in combination with snow and/or water coupling, as there must already be a thermal gradient between the tiles before it can have an effect. Finally, the lateral heat and water fluxes will depend on the geometry of the system, in particular the distance parameter (D).

#### 4.2 Distance parameter (D)

At the peat plateau location, we test performed how a sensitivity analysis the system is to of the distance parameter (D), we perform another sensitivity test for the mire location. As seen from Eq. (5) and (6), both which determines lateral water and heat fluxes depend linearly in on this parameter in an inverse proportional fashion (Eq. (5) and (6)). However, the water has the potential for can potentially draining fast, and, with soil water contents becoming in quickly reaching equilibrium, while the heat conduction is generally much slower and remove temperature differences less efficiently. To test a wide range of parameter values, we simulate a larger system than in section 3, we. Again, we simulate a circular elevated tile (as in Sect. 3), but scale both the elevated PPLAT and the surrounding MIRE by a factor of 100 in each horizontal direction, and testing length scales from 0.2 m to 500 m.

Figure 11 shows the resulting surface elevation in the peat plateau (a), as well as the lateral heat (b) and water fluxes (c) shown as 10-year running averages. Here we see that for the most part larger distance parameters correspond to earlier permafrost thaw/melt and ground subsidence. This is clearly a water effect, as the simulated annual horizontal heat flux (HHF) is small, (and scale in almost linearly with  $D^{-1}$ ) and snow redistribution does not depend on this parameter. Hence the main mechanism appears to be that larger D gives leads to lower lateral water fluxes and hence a higher soil moisture and larger soil thermal conductivity at PPLAT. Only with very small or large D is this picture reversed. Going Increasing from the distance parameter off from 0.2 m to 0.5 m gives instead results in a slight delay in degradation, as. For such small values of D, the changes in lateral heat fluxes are become important for such small values of D, whereas while lateral water

~~redistribution~~ water fluxes occur ~~are~~ almost instantaneously and ~~does~~ not change noticeably. Hence the effect is so that that larger values of  $D$  ~~gives~~ lead to a slower degradation. In the other end of the simulated range, degradation is also delayed when ~~going increasing~~  $D$  from 50 m to 100 m, and further to 500 m. ~~With such large D values~~ In these cases, the drainage is much slower, ~~and, so that~~ full drainage on the annual time scale is no longer realized. Hence ~~Therefore~~, other processes like ~~the higher~~ increased heat capacity ~~due to from~~ increased soil moisture might be more important than the conductivity effect of reduced drainage.

~~While this does not translate directly to the effect of changing size of the PPLAT tile,~~ This sensitivity analysis ~~shows what highlights~~ the importance of different ~~two lateral subsurface processes are important~~ lateral fluxes on different scales, ~~showing suggesting~~ that the ~~results from the previous section~~ effect of laterally coupled tiles strongly depends strongly on the geometries and sizes of the ~~landscape~~ structures ~~represented~~.

## 5. Discussion

With a relatively simple two-tile system, we have been able to simulate observed microtopographic changes associated with ~~degradation of~~ ice-rich permafrost ~~degradation~~. ~~As a direct effect, we have seen that this altered~~ The introduction of laterally coupled tiles influenced both the mean soil temperatures, active layer thicknesses, timing of permafrost degradation, soil moisture conditions and the surface energy balance fluxes. In the following, we ~~will~~ discuss limitations and sources of errors in the current study (5.1), ~~how this method might be~~ implemented ~~ationed~~ in large-scale models (5.2), and possible implications for ~~simulations simulating of~~ the PCF (5.3).

### 5.1 Limitations and sources of errors

The method applied here is by design a minimalistic approach to include ~~the~~ important lateral processes in permafrost landscapes, ~~where keeping~~ the number of new parameters (see Fig. 3) ~~have been kept~~ at a minimum. As capturing the detailed properties at the two ~~specific~~ test sites ~~locations has have~~ not been the objective of this study, the different model parameters have not been fine-tuned, neither for the default NoahMP model ~~nor~~ the new tile geometry parameters. As noted ~~above~~ in Sect. 3, there are differences between ~~simulations and observations for both locations~~ the observed properties at the two locations, ~~and what is simulated here~~. In particular, the simulations showed considerably warmer permafrost temperatures and a larger Bowen ratios at Samoylov Island, ~~whereas while~~ the peat plateau at Suossjavri appears more stable in the simulations ~~than what is observed~~ compared to observations (Borge et al., 2017). In the following, we ~~will~~ discuss ~~some~~ aspects of the two-tile system that were found to be particularly important for our simulations, as well as ~~other properties~~ and processes ignored ~~herein the model setup, which,~~ ~~which~~ These might explain ~~some of the these~~ discrepancies ~~between our simulations and what is observed at these sites~~. However, given the relatively coarse resolution of the forcing data, a certain disagreement must be expected.

*Snow:* ~~First,~~ ~~the~~ The minimum snow depth ( $H_{Smin}$ ) was found to be a key parameter. As seen in Fig. 10, the timing of the degradation at both locations ~~were was~~ sensitive to the snow redistribution. ~~This was further confirmed with the sensitivity~~

simulations exploring different  $H_{s_{min}}$  values, and ~~This~~ is in agreement with previous studies on the effect of the seasonal snow cover snow on the thermal regime (e.g. Ginsås et al., 2016). ~~For In~~ our simulations, ~~it was found that a~~ higher minimum snow accumulation limit was needed for the peat plateau (10 cm) than for the polygonal site (5 cm); in order to simulate stable conditions in the beginning of the simulation and degradation within the current century. We note that the end-of-winter snow depths at both locations are within the observed range; ~~and that different~~ the  $H_{s_{min}}$  values mainly affects the timing of initial permafrost thaw. In the future, ~~Ideally~~, this value should ideally ~~in the future~~ be linked to surface characteristics, such as the like-vegetation height. ~~However, this parameter should in the future be studied further, and ideally be linked to simulated properties like vegetation height.~~

*Excess ice initialization:* Another key aspect of the ~~coupled two-tile~~ system is how the excess ice is ~~initiated~~ initialized, in particular ~~the~~. ~~The~~ depth at which the excess ice ~~was is~~ inserted in the soil column ( $Z_{extop}$ ) ~~could in theory be set to the observed ALT.~~ ~~T~~Test simulations revealed, ~~however~~, that inserting the excess ice this at a too large or too shallow depths ~~would result~~ in ~~either~~ a too stable or too unstable dynamic system, respectively. ~~Inserting this~~ Setting  $Z_{extop}$  at the depth of the simulated ALT was ~~therefore~~ found ~~to be important to simulate~~ produce reasonable ~~degradations~~ results, while inserting the excess ice below the observed ALT, resulted in immediate excess ground ice melt, as the active layer thickness was overestimated for both locations (Sect. 3). Likewise, the density-volumetric fraction of the excess ground ice is important for how fast the system evolves once degradation starts; ~~and~~ ~~At~~ the polygonal tundra site, ~~what this in particular determines is~~ the ~~the~~ new stable state after excess ice thaw in RIM, as it determines how fast an excess ice-free buffer layer can form. The values used here in the simulations ~~is are~~ to some extent based on observations and expert judgement, but still a certain degree of trial and error was needed, in particular to simulate a stable trough at the tundra site, without a continued, unrealistic deepening of the RIM tile.

*Soil properties:* An important limitation in the current model system is the uniform soil properties, both with respect to depth and between the tiles. This is a simplification inherent in the current NoahMP model, which does not consider different soil types at different depths, including which included also our implementation of organic fractions. This meant that in order to represent observed soil properties near the surface, in particular the high porosity typical for peat, we likely had to accept also simulated too large porosities deeper into in the soil. The effect of this is that ~~As a consequence,~~ too much soil water is undergoes a phase change ~~changing phase at the bottom of the in the~~ active layer ~~every year~~, dampening the temperature signal from the surface. ~~Another effect might be that~~ In addition, as the initial amount of soil (pore) ice is too large, too much the energy might be needed to thaw the soil ~~might be exaggerated, as the initial amount of soil (pore) ice is too large.~~ Also related to soil properties, ~~Furthermore, formation of new is the lack of new~~ excess ice ~~formation and~~ is not represented in the model, as well as of explicit representation of surface water above the soil column. ~~both of which might act to slow down degradation.~~ While appropriate model formulations are lacking for the former ~~is a more uncertain process for which appropriate model formulations are lacking~~, the latter has been accounted for in ~~the a~~ companion paper (Nitzbon et al., 2018) using a more dedicated permafrost model.

*Larger scale hydrology:* As shown in ~~the companion paper~~ (Nitzbon et al., 2018), the hydrological setting surrounding hydrology is within the larger-scale drainage regime is important for the stability of permafrost in polygonal tundra. ~~Here In~~

~~this study, we have simulated one hydrological setting, where~~ surface water is removed as runoff, ~~but otherwise the polygon is detached from the surroundings~~ which corresponds to a single (possible rather artificial) hydrological setting. Observations from Samoylov Island reveals, ~~however,~~ that very different hydrological conditions can be found even on this relatively small island. Simulating ~~instead~~ surface water in low-centered polygons, or water-filled troughs in the degraded, high-centered stage, ~~would~~ would likely modify the results ~~presented here through reduced albedo, increased heat conduction and lower snow redistribution due to smaller elevation differences between the tiles.~~ Results from model simulations, which ~~including~~ take larger-scale hydrology into account ~~these processes,~~ show increased soil ALT and earlier permafrost degradation when standing water is included (Langer et al., 2016; Nitzbon et al., 2018).-

*Vegetation:* Another factor ~~not considered in this study that could modify the results~~ is the influence of vegetation, ~~which has not been considered here.~~ In particular, the appearance of new vegetation in troughs ~~might is likely to~~ lead to an increased insulation, and act as a negative feedback to the degradation of the polygons, while also interacting ~~also~~ with the local hydrology.

*Other lateral processes:* Finally, ~~we note that~~ there are other lateral processes ~~that we have~~ not accounted for, ~~including such as~~ lateral erosion and heat advection associated with lateral water flow. ~~While we have included the effect of lateral heat flux on the average temperature, this heat flux will in reality often lead to permafrost thaw and erosion near the margins.~~ Lateral erosion is a complex process, which likely requires accounting for the heat input along the (vertical or inclined) erosion surface, which cannot be included in the presented model scheme in a straight-forward fashion. Furthermore, our simulation only includes lateral water flux near the surface, ~~whereas~~ while a number of studies have demonstrated that deeper water movement and related heat advection might affect soil thermal conditions (Kurylyk et al., 2016; Sjöberg et al., 2016). Both of these processes ~~likely might play a role~~ contribute to for the degradation of peat plateaus currently observed in Northern Norway.

Despite these limitations, In summary, we have seen that ~~Despite these limitations, our~~ results ~~show suggest~~ a major improvement in terms of representing current permafrost conditions at the two locations, ~~despite these limitations, and will help improve permafrost processes in LSMs particularly on lateral transport, with~~. The discrepancies with in-situ current observations ~~are~~ consistently smaller for the laterally coupled simulation compared to REF. Considering ~~also that observations from both locations show considerable~~ the documented spatial variability of the permafrost ground thermal regime, ~~and current temperatures at the polygonal site is rapidly increasing,~~ we consider these differences acceptable to be modest, mainly influencing the timing of the future permafrost degradation. Nevertheless, adding further key processes to the two-tile system ~~Further is likely to improvements and added realism could be expected by~~ improve the simulation results ~~adding more processes to the two tile system.~~ Here, we highlight consider the representation of standing water as the most important process ~~we consider to be of highest priority,~~ followed by representation of ~~Furthermore, some of the biases seen here could be mitigated with~~ vertically varying organic fractions and soil types, ~~and as well as as well as~~ dynamical vegetation. Most of these are, ~~which is~~ already included in several large-scale LSMs (e.g. Lawrence et al., 2011; Reick et al., 2013).

## 5.2 Interactive tiling in coupled ESM simulations?

Having demonstrated and discussed the large impact lateral fluxes may have on the simulated permafrost state and evolution we turn to the possibilities for representing these processes in global-scale ESMs. Here, In this study, we have used NoahMP as a test model, in which the representation of subsurface processes is ~~are represented~~ comparable to LSMs used for global climate simulations. In ~~the a~~ companion study, Nitzbon et al. (2018) ~~have~~ demonstrated that the same basic method can be utilized in a completely different model, which suggests that the method is ~~model-independent~~ of the individual model setup. Implementation in a large-scale LSM, also with full biogeochemistry, should therefore ~~be more of a rather be a~~ technical ~~rather~~ than a conceptual challenge, as is applying the modified model online in an ESM framework. From the theoretical side, the challenge is mainly the scale gap between the small-scale units considered here (on the order of 10 – 100 m) to the 100-km scale typical for current global simulations. However, as mentioned in ~~section-Sect.~~ 2.3, the concept of self-similarity offers the possibility to represent larger landscapes with a small set of laterally coupled units.

As the simplest implementation, ~~we suggest using~~ the two-tile structure outlined here in this study to could represent a fraction of a grid-cell in a large-scale model, alongside the default LSM simulation. Using for instance the maps from Olefeldt et al. (2016) ~~to identify areas of ice-rich permafrost susceptible to thermokarst development,~~ areas of ice-rich permafrost these could can be represented by a separate land unit consisting of two laterally coupled tiles. Ground ice data from Brown et al. (1998) could provides a starting point here, which was also used similar to in the study by Lee et al. (2016). In the simplest form, this would require only some representative geometries for each type of permafrost landscape. Assigning excess ground ice to the first soil layers below the simulated ALT is in our view has been a reasonable first-order choice for the two test sites, but this procedure is likely not adequate for areas with excess ice well below the current active layer, e.g. due to burial or melting of excess ground ice in the past (e.g. truncated ice wedges, Brown, 1967). Ultimately, new global data sets for ground ice depth, whereas excess ice density – and the geometries for of the two tiles must be compiled, for example building on approaches as in Hugelius et al, (2014) and Strauss et al., (2017). Nevertheless, even with Even with relatively crude estimates of representative geometriesthese parameters in each permafrost region, the proposed method would this would for the first time allow including the effects of lateral heat, moisture and snow fluxes on permafrost degradation in global models. As suggested by field observations (Liljedahl et al., 2016), these can have substantial effects on the evolution of the permafrost region which cannot be represented when assuming homogeneous permafrost and ice distributions.

The method described here is, however, not limited to a two-tile structure. As demonstrated by Nitzbon et al. (2018), the same basic formulation can be applied also with three tiles, and with water exchange with an external reservoir. In such a configuration, the coupling method already gives a substantially higher level of ~~complexity and~~ realism for the specific site studied (Samoylov Island), although the number of input parameters is correspondingly increased. From a system with three coupled tiles, one ~~can could~~ expand the method further to more coupled tiles representing physical locations in a single system (like surrounding hills or waterbodies), or to an ensemble of two- or three-tile systems with different geometries within a single grid cell. However, with the computational cost of current LSMs used in ESMs, this ~~would is likely relatively quickly to~~ become a large computational burden.

— Regardless of the choice of implementation, the method proposed here should be considered in the context of a larger effort to improve the representation of horizontal land processes in ESMs. The land component of coupled atmosphere-land surface models has typically been of considerable complexity in the vertically complex dimension, but includes little horizontal interaction and variation (see e.g. Clark et al., 2015). While representing heterogeneous excess ice is a relevant only in certain regions, we believe that a more flexible model structure with individual sub-grid soil columns that can exchange water and snow is a concept that deserves further investigation also in other regions.

### 5.3 Interactive tiling to improve simulations of future permafrost-carbon-feedback?

Improved representation of the PCF is a key motivation for the model developments outlined herein in this study. In the following, and we will therefore in the following discuss the prospects qualitatively how it might be affected by the geophysical changes seen here, of a coupled tile structure in LSMs with respect to simulations of carbon turnover in permafrost regions.

As a first order effect, the PCF depends on how much, and when at what time, currently frozen ground is thawed and soil carbon exposed to microbial decomposition. As substantial changes in permafrost state (e.g. Fig. 5) and timing of degradation (Fig. 4 and 7) have been demonstrated here, it is clear that also the simulated PCF will be affected by implementing this method in a fully coupled ESM. The CMIP5 ensemble of climate models showed drastically different permafrost areas (Koven et al., 2013a), which have been a major contribution to the uncertainty in the PCF. More recent simulations with improved ESMs (McGuire et al., 2018) still show significant differences in simulated PCF and vegetation response in the permafrost region. This is despite the fact that they all still lack the representation of kind of sub-grid processes included here. Our results therefore suggest that the lack of lateral processes that currently in current large-scale LSMs used in climate models might also have could potentially contribute to large biases in the amount of permafrost area and when it could thaw due to the lack of lateral processes discussed here timing of thawing (e.g. Rowland et al., 2015).

On top of this Furthermore, our method shows a non-linear behavior and thresholds that are not found in the reference simulation. Both the polygonal tundra and peat plateau settings show display more stable conditions when lateral fluxes are included, before relatively rapid changes were initiated. One reason for this, is the non-linear effect of the snow cover on the insulation of the soil-ground during winter. When considering a grid-cell mean-averaged snow depth, the effect of slightly increased or decreased snow accumulation is often generally small. However, in a laterally coupled system where in which snow redistribution depends on dynamical micro-topography, even a small increase in snow accumulation can be enough to initiate-trigger a change. Once elevated features begin to degrade, they more snow begins to accumulate, so that the changes cannot be reversed, and may not even stabilize before reaching a new state, even if the initial changes in snow accumulation were temporary. This kind of behavior irreversible behaviour has should be investigated in more detail implications for for so-called overshoot scenarios, which is being discussed in relation which are discussed in the context of the more ambitious mitigation scenarios (Comyn-Platt et al., 2018).

Accurate simulation of the PCF depends also on the soil moisture conditions under which permafrost thaws and carbon is mobilized. This has been demonstrated both in laboratory measurements studies (Elberling et al., 2013; Schädel et al., 2016; Knoblauch et al., 2018) and model simulations (Lawrence et al., 2015), showing that a realistic simulation of local

hydrology is important for ~~PFC-PCF~~ simulation. Our results here capture key soil moisture conditions observed in the two ~~kinds of simulated permafrost~~ landscapes ~~simulated~~, which cannot be represented in the reference simulation. Furthermore, our method simulates the rapid transitions in soil moisture conditions that are associated with thermokarst development, which might in itself be an important factor for the amount and partitioning (CO<sub>2</sub> vs CH<sub>4</sub>) of carbon release to the atmosphere. Incubation ~~measurements-experiments~~ have shown that the largest greenhouse gas production from thawing permafrost could be realized when previously wet soil was decomposed under drained conditions (Elberling et al., 2013). This is exactly the process observed in the centers when LCP transition ~~into-to~~ HCP, which again ~~demonstrates-suggests~~ that the processes included here might play an important role ~~in accurately simulating PFC-for simulating permafrost carbon turnover~~.

Finally, ~~the sub-gridlaterally coupled~~ tiling ~~proposed here~~ will likely impact dynamical vegetation modeling in the permafrost region, which is important for understanding the future carbon signal from this region. Both greening and browning of the Arctic have been observed ~~over-in~~ the recent past ~~and both could be expected also in the future~~, although ~~models predict~~ a general greening and increased carbon storage in vegetation ~~is what models are predicting~~ (McGuire et al., 2018). ~~Representing sub-grid variability in snow and soil conditions in conjunction with a dynamical vegetation model might contribute to simulate future vegetation changes more accurately, e.g. by representing frost damage at locations with shallow snow cover (Phoenix and Bjerke, 2016)The processes related to PFT migration and competition might, however, be different when the sub-grid variability in snow and soil conditions represented here are included.~~ This further exemplifies ~~the potential of laterally coupled tilinghow the method applied here might offer new details and added realism whenfor~~ simulating land-atmosphere interactions in the Arctic permafrost region ~~in a more realistic fashion~~.

## 6. Conclusions

~~Here-In this study, we have-simulated~~ dynamically changing microtopography and related lateral fluxes of snow, water and heat ~~in permafrost landscapes with using~~ a two-tile model approach, ~~and applied it to two very different kinds of permafrost landscapes. The model is tested for polygonal tundra in the continuous and peat plateaus in the sporadic permafrost zone, representing two highly different permafrost landscapes dominated by ice-rich ground.~~ The main findings of our investigation are as follows:

1. Currently observed degradation processes in both polygonal tundra and peat plateaus could be simulated with a simple tiling approach accounting for changing micro-topography and small-scale lateral fluxes. This included representing the transition from low- to high-centered polygons and the transition from a stable to degrading peat plateau in the sporadic permafrost zone.
2. The timing and speed of degradation at the polygonal site differed strongly between the ~~two-tile model and reference simulations with a classic model using only a single tiletwo simulations~~. Whereas reference simulation showed slow, but ~~continuing-consistent~~ degradation ~~which did not stabilize during the simulation~~, the ~~laterally~~ coupled tiles showed a delayed onset of permafrost degradation, followed by a more rapid ice melt and subsidence, before the system stabilized in a new state with an elevated, dry center and wet trough.

3. Deep soil temperatures differed substantially between the reference simulation and the two-tile system. For the polygonal tundra site ~~at Samolylov Island, the~~ simulated temperatures at approximately 13 m depth ~~was/were~~ about 2 °C colder with coupled tiles ~~in the current climate~~ compared to the reference simulation.
4. The two-tile model was capable of representing ~~D~~ dry near-surface soil conditions in the elevated features ~~could be represented~~ at both locations, with substantial effect on surface energy balance fluxes.
5. Sensitivity studies showed that lateral fluxes of snow, water and heat all affected the stability of the permafrost at both locations, with their relative contribution depending on the distance parameter.

These results show that lateral fluxes and changing microtopography have a strong impact on simulated permafrost extent and conditions. Together with ~~the a~~ companion study by Nitzbon et al. (2018), we ~~have demonstrated~~ that ~~this laterally coupled tiles facilitate a simple and computationally effective first-order representation for a range of observed degradation processes in ice-rich permafrost areasean be realized to a first order with a simple and computationally effective tiling approach~~. Applying the proposed method in land surface models with full biogeochemistry shows significant potential to drive simulations of the permafrost-carbon-feedback towards reality.

*Code availability.* The NoahMP model code is available at <https://github.com/NCAR/hrldas-release>. Modifications to the code implemented here are available from the corresponding author upon request.

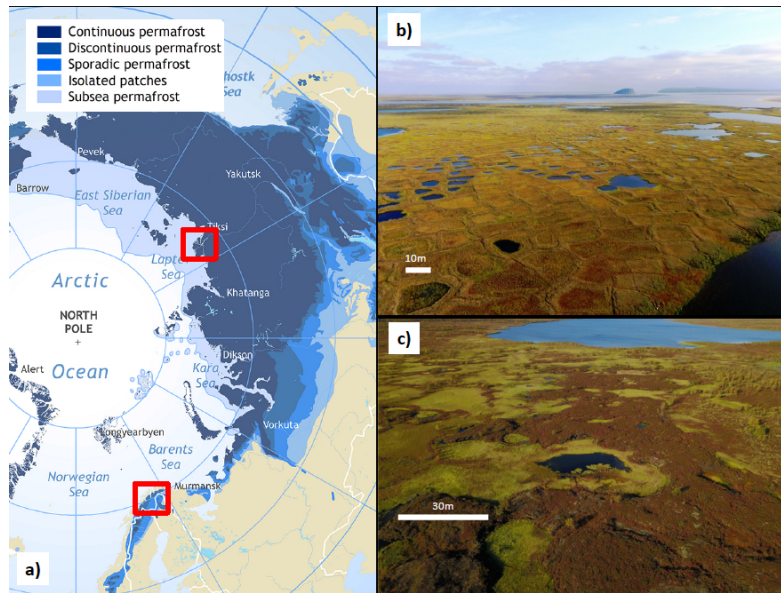


**Figure 1:** a) Location of the two test sites on top of the map of permafrost distribution in the Arctic (Brown et al. 1998). b) example of low-centered polygons on Samoylov Island, Northern Siberia (Photo: Sebastian Zubrzycki). c) Example of peat plateau near Suossjavri, Northern Norway (Photo: Sebastian Westermann). The two sites are located in the continuous and sporadic permafrost zones, respectively.

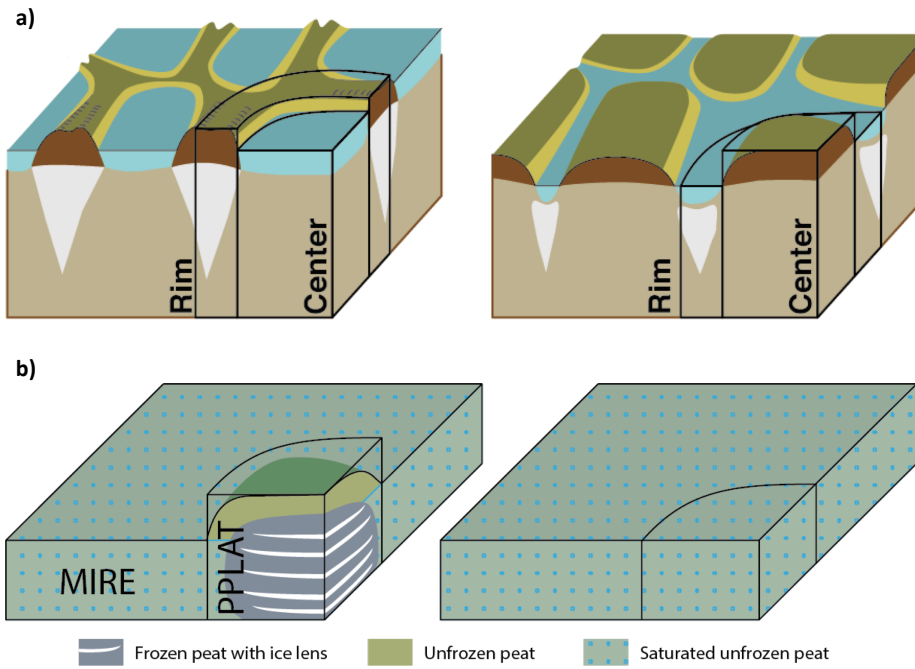


**Figure 2: a) Schematic presentation of undegraded, low-centred polygon (left) and degraded, high-centred polygons (right) with corresponding tiles used in this study (adapted from Liljedahl et al. 2016). b) Schematic presentation of peat plateau in a surrounding mire (left), and the mire after the peat plateau has degraded (right), with corresponding tiles.**

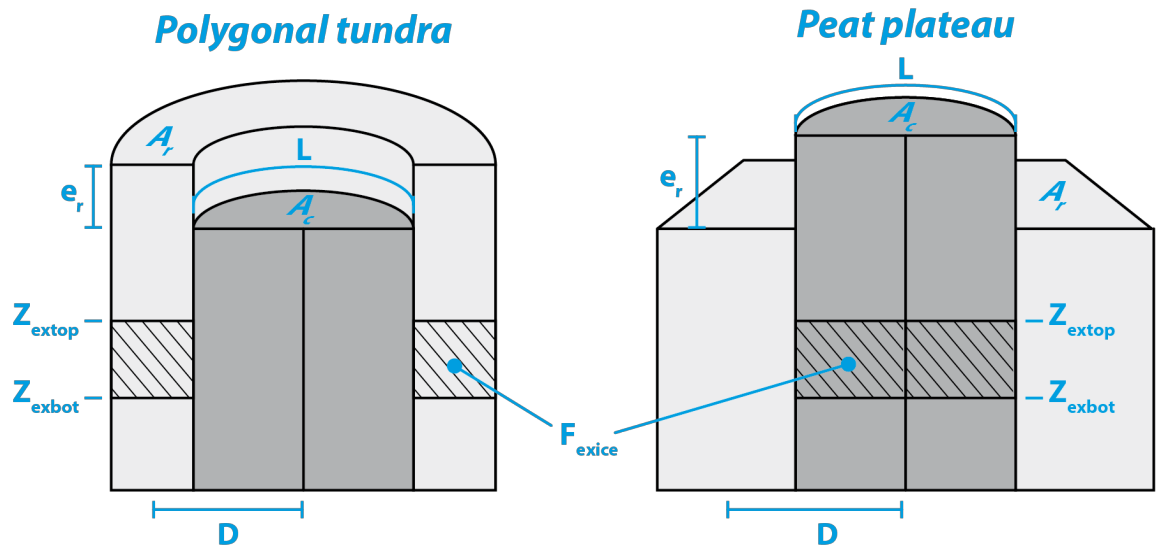


Figure 3: Schematic presentation of the two-tile system with geometry parameters. Parameter values used for the two locations are listed in Table 1.

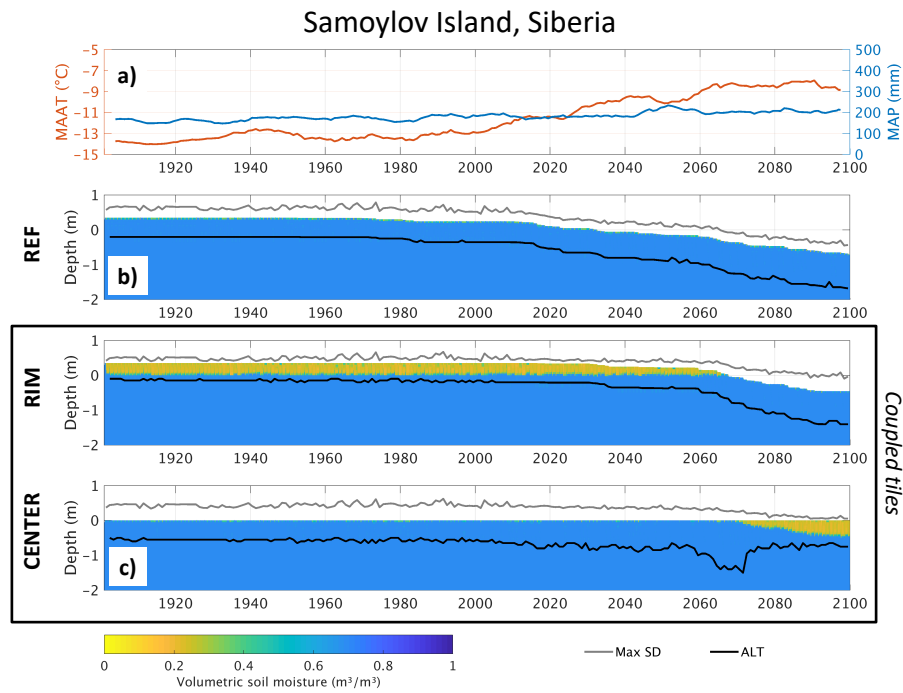
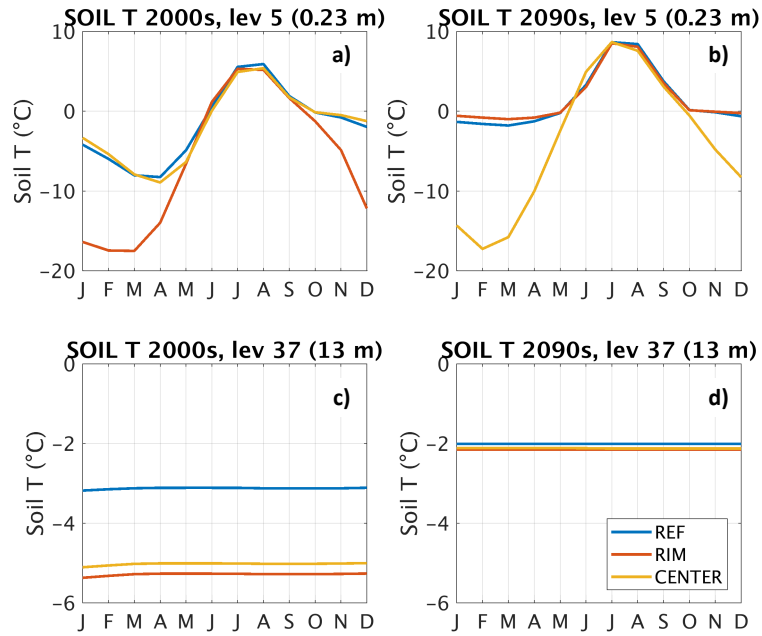


Figure 4: a) 10-year running average of mean annual air temperature (MAAT) and mean annual precipitation (MAP) at Samoylov Island. Soil moisture and surface elevation are shown as colored region in b) reference simulation, c) and in the **laterally** coupled tiles. Note that both the surface elevation (relative to the CENTER tile) and the unsaturated soil (orange and green colors) change in the coupled tiles as excess ice melts and the lateral fluxes changes. -Maximum annual snow depth (MaxSD) and active layer thickness (ALT) are shown as gray and black lines, respectively.



**Figure 5: Average annual temperature cycle during first (a, c) and last (b, d) decade of 21<sup>st</sup> century at Samoylov Island, in the 5<sup>th</sup> model layer (a, b; 0.23 m below surface) and the 37<sup>th</sup> model layer (c, d; approximately 13 m below reference height). See layer depths in Fig. A1a.**

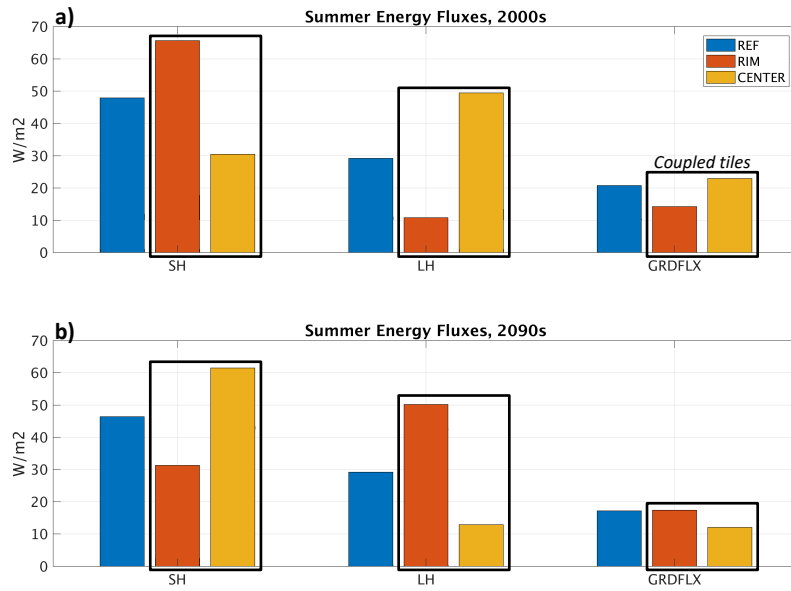


Figure 6: Summer surface energy fluxes at Samoylov Island during first (a) and last (b) decade of the 21<sup>st</sup> century in reference simulation (REF) and laterally coupled tiles (RIM and CENTER). ~~HFXSH~~: sensible heat flux, LH: latent heat flux, GRDFLX: ground heat flux.

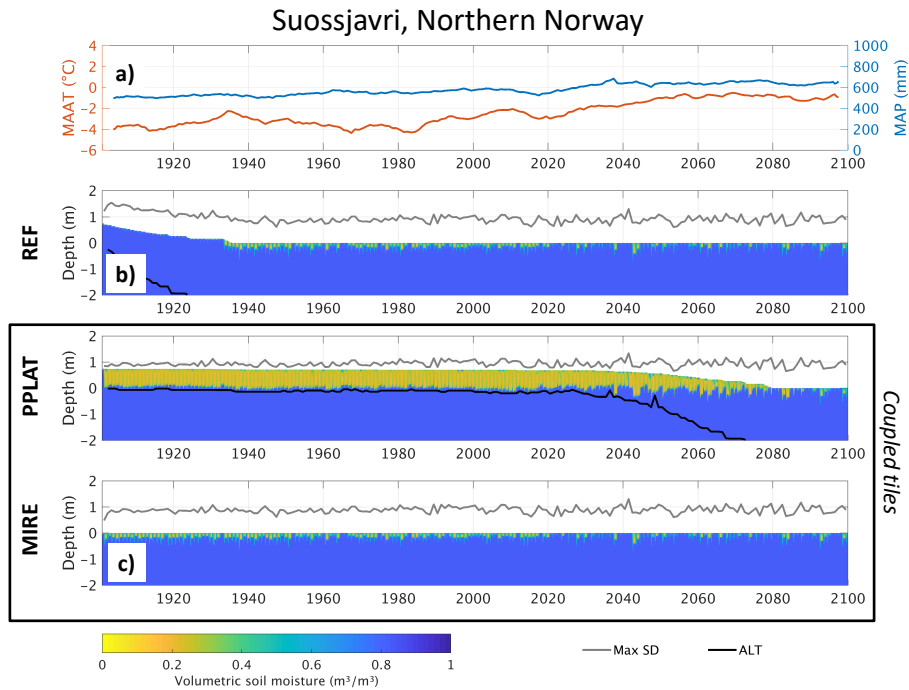
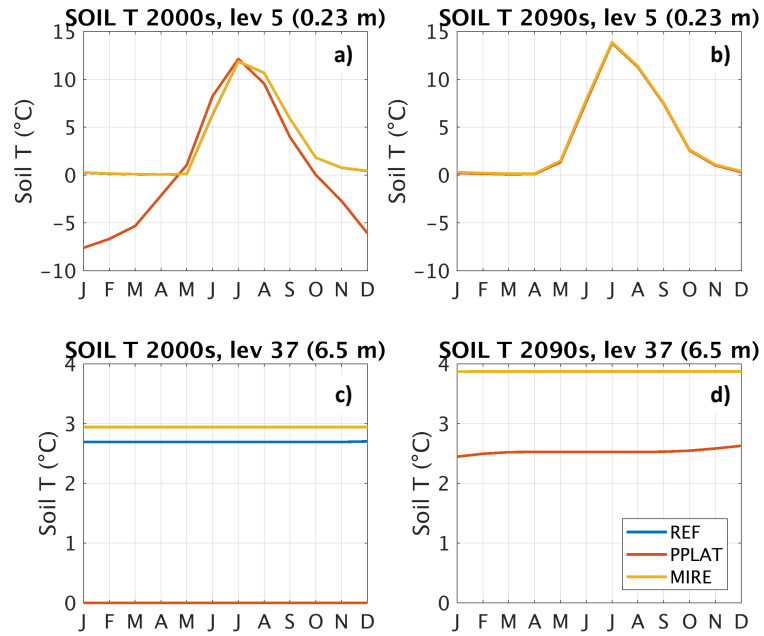
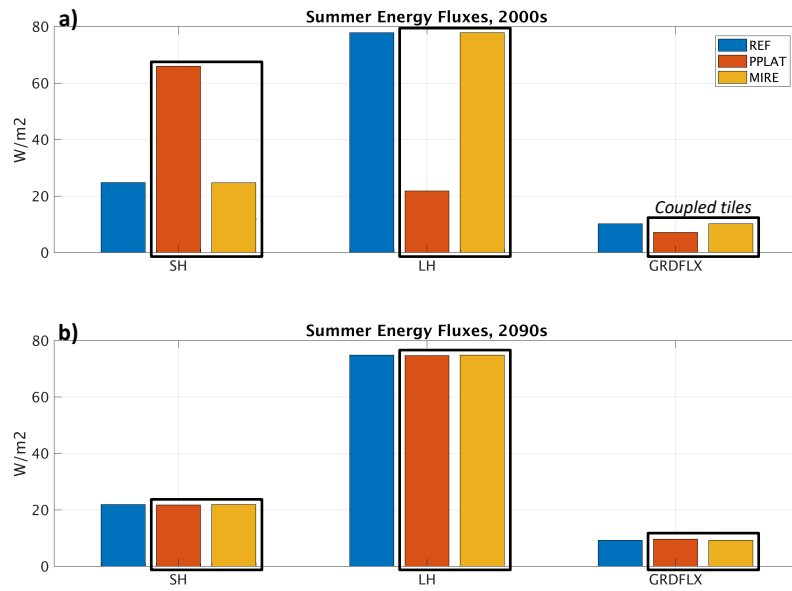


Figure 7: a) 10-year running average of mean annual air temperature (MAAT) and mean annual precipitation (MAP) at Suossjavri, Northern Norway. Soil moisture and surface elevation are shown as colored region in b) reference simulation, c) and in the **laterally** coupled tiles. Note that both the surface elevation (relative to the CENTER tile) and the unsaturated soil (orange and green colors) change in the coupled tiles as excess ice melts and the lateral fluxes changes. -Maximum annual snow depth (MaxSD) and active layer thickness (ALT) are shown as gray and black lines, respectively.



**Figure 8: Average annual temperature cycle during first (a, c) and last (b, d) decade of 21<sup>st</sup> century at Suissjavri, Northern Norway, in the 5<sup>th</sup> model layer (a, b; 0.23 m below surface) and the 37<sup>th</sup> model layer (c, d; 6.5 m below reference height). See layer depths in Fig. A1b.**



**Figure 9: Summer surface energy fluxes at Suossjavri, Northern Norway, during first (a) and last (b) decade of the 21<sup>st</sup> century in reference simulation (REF) and laterally coupled tiles (RIM and CENTER). ~~HFXSH~~: sensible heat flux, LH: latent heat flux, GRDFLX: ground heat flux.**

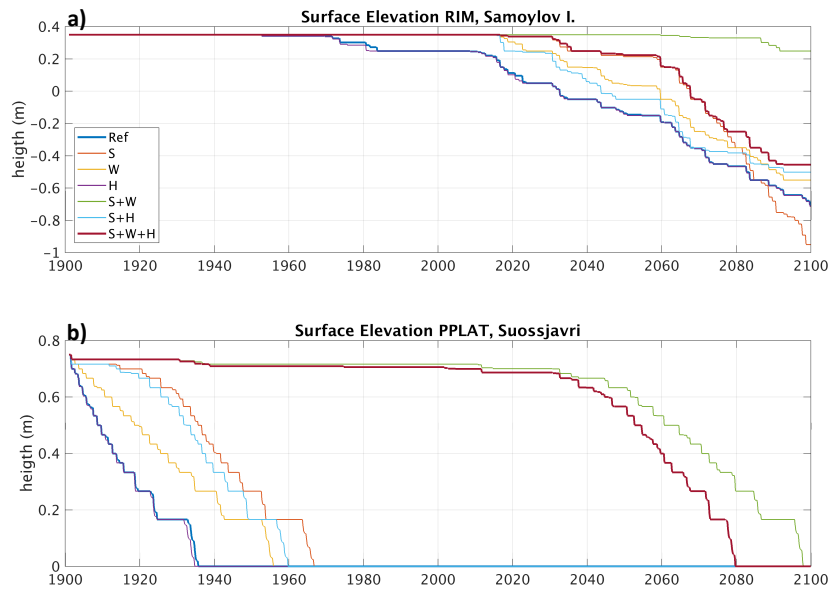


**Figure 10: Surface elevation of RIM relative to CENTER at Samoylov Island, Siberia (a), and of PPLAT relative to MIRE at Suossjavri, Northern Norway (b) for different combinations of lateral fluxes. Thick blue line represents reference simulations (REF; no lateral fluxes), and thick red line represents fully coupled two-tile simulation. S: snow, W: water, H: heat.**

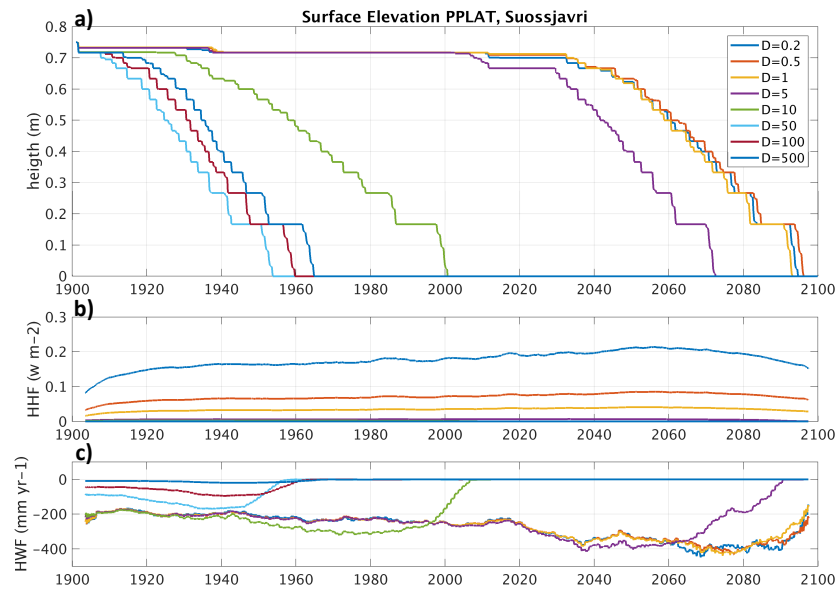


**Figure 11: Surface elevation of PPLAT at Suossjavri, Northern Norway (a) for different values of distance parameter (D) between the two interacting tiles, and corresponding horizontal heat flux (HHF; b), and horizontal water flux (HWF; c). Note that the area of PPLAT is different (larger) here than in the standard simulations (Fig. 7), giving a different evolution for the same (D=10) distance parameter.**

Location:	$A_r(m^2)$	$A_c(m^2)$	L(m)	D(m)	e(m)	$Z_{extop}(m)$	$Z_{exbot}(m)$	$F_{exice}$ (%)
Sam	39.3	39.3	22.2	4.27	0.35	0.55	2.8	66.7
Suo	9.92e3	78.5	31.4	10.0	0.75	0.75	3.75	25.0

**Table 1: Tile geometry and excess ice distribution. See detail in Fig 3.**

Location:	OrgF(%)	Scenario	$T_0(^{\circ}C)$	$H_{S_{min}}$ (m)	$P_{scale}$	Soil type
Sam	50	RCP4.5	-9.0	0.05	0.6	Silt
Suo	80	RCP4.5	0.0	0.1	1.0	Silt

**Table 2: Soil properties and initial conditions.**

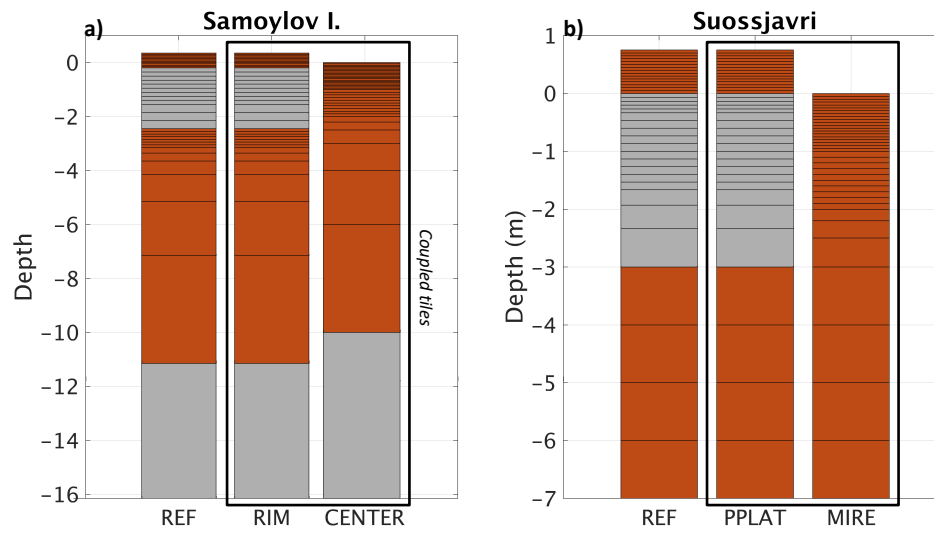


**Figure A1: Vertical resolution and at Samoylov Island (a) and Suossjavri (b). Gray colours indicate layers initialized with excess ice. Excess ice initiated in bottom layer at Samoylov Island is used to adjust the rim height ( $e_r$ ) independently of near-surface excess ice.**

*Author contributions.* KSA and SW designed the study. KSA implemented the code, carried out the simulations and wrote the manuscript. LM made Fig. 2 and Fig 3. All authors interpreted the results and contributed to the manuscript. SW and HL secured the project funding.

*Competing interests.* JB and ML are members of the editorial board of The Cryosphere. All other authors declare that they have no conflict of interest.

*Acknowledgements.* The authors gratefully acknowledge the support of the Research Council of Norway for the PERMANOR project (no. 255331) and FEEDBACK project (no. 250740), support from the strategic research initiative LATICE (Faculty of Mathematics and Natural Sciences, University of Oslo <https://mn.uio.no/latice>), as well as simulation resources provided by NOTUR (project no. NN9489K) and the Department of Geosciences, UiO. [-We would also like to thank the two anonymous reviewers for valuable suggestions and feedback.](#)

## References

- Aas, K. S., Gisas, K., Westermann, S., and Berntsen, T. K.: A Tiling Approach to Represent Subgrid Snow Variability in Coupled Land Surface-Atmosphere Models, *Journal of Hydrometeorology*, 18, 49-63, 10.1175/Jhm-D-16-0026.1, 2017.
- Aune, B.: Temperaturnormaler, normalperiode 1961-1990, *Nor. Meteorol. Inst. Rapp. Klima*, 1993, 1-63, 1993.
- Beer, C.: Permafrost Sub-grid Heterogeneity of Soil Properties Key for 3-D Soil Processes and Future Climate Projections, *Front Earth Sci*, 4, UNSP 81, 10.3389/feart.2016.00081, 2016.
- Bisht, G., Riley, W. J., Wainwright, H. M., Dafflon, B., Yuan, F. M., and Romanovsky, V. E.: Impacts of microtopographic snow redistribution and lateral subsurface processes on hydrologic and thermal states in an Arctic polygonal ground ecosystem: a case study using ELM-3D v1.0, *Geosci Model Dev*, 11, 61-76, 10.5194/gmd-11-61-2018, 2018.
- Boike, J., Wille, C., and Abnizova, A.: Climatology and summer energy and water balance of polygonal tundra in the Lena River Delta, Siberia, *Journal of Geophysical Research*, 113, <https://doi.org/10.1029/2007JG000540>, <http://doi.wiley.com/10.1029/2007JG000540>, 2008.
- Boike, J., Kattenstroth, B., Abramova, K., Bornemann, N., Chetverova, A., Fedorova, I., Frob, K., Grigoriev, M., Gruber, M., Kutzbach, L., Langer, M., Minke, M., Muster, S., Piel, K., Pfeiffer, E. M., Stoof, G., Westermann, S., Wischnewski, K., Wille, C., and Hubberten, H. W.: Baseline characteristics of climate, permafrost and land cover from a new permafrost observatory in the Lena River Delta, Siberia (1998-2011), *Biogeosciences*, 10, 2105-2128, 10.5194/bg-10-2105-2013, 2013.
- Boike, J., Nitzbon, J., Anders, K., Grigoriev, M., Bolshiyarov, D., Langer, M., Lange, S., Bornemann, N., Morgenstern, A., Schreiber, P., Wille, C., Chadburn, S., Gouttevin, I., and Kutzbach, L.: A 16-year record (2002-2017) of permafrost, active layer, and meteorological conditions at the Samoylov Island Arctic permafrost research site, Lena River Delta, northern Siberia: an opportunity to validate remote sensing data and land surface, snow, and permafrost models, *Earth System Science Data Discussions*, pp. 1-77, <https://doi.org/https://doi.org/10.5194/essd-2018-82>, <https://www.earth-syst-sci-data-discuss.net/essd-2018-82/>, 2018.
- Borge, A. F., Westermann, S., Solheim, I., and Etzelmüller, B.: Strong degradation of palsas and peat plateaus in northern Norway during the last 60 years, *The Cryosphere*, 11, 1-16, 10.5194/tc-11-1-2017, 2017.
- [Brown, J.: Tundra Soils Formed over Ice Wedges Northern Alaska, \*Soil Sci Soc Am Pro\*, 31, 686-&, DOI 10.2136/sssaj1967.03615995003100050022x, 1967.](https://doi.org/10.2136/sssaj1967.03615995003100050022x)
- Brown, J., Ferrians Jr, O. J., Heginbottom, J., and Melnikov, E.: Circum-Arctic map of permafrost and ground-ice conditions, National Snow and Ice Data Center/World Data Center for Glaciology, Boulder, CO, 1998.
- Burke, E. J., Dankers, R., Jones, C. D., and Wiltshire, A. J.: A retrospective analysis of pan Arctic permafrost using the JULES land surface model, *Clim Dynam*, 41, 1025-1038, 10.1007/s00382-012-1648-x, 2013.
- Chadburn, S., Burke, E., Essery, R., Boike, J., Langer, M., Heikenfeld, M., Cox, P., and Friedlingstein, P.: An improved representation of physical permafrost dynamics in the JULES land-surface model, *Geosci Model Dev*, 8, 1493-1508, 10.5194/gmd-8-1493-2015, 2015.
- Chadburn, S. E., Krinner, G., Porada, P., Bartsch, A., Beer, C., Marchesini, L. B., Boike, J., Ekici, A., Elberling, B., Friborg, T., Hugelius, G., Johansson, M., Kuhry, P., Kutzbach, L., Langer, M., Lund, M., Parmentier, F. J. W., Peng, S. S., Van Huissteden, K., Wang, T., Westermann, S., Zhu, D., and Burke, E. J.: Carbon stocks and fluxes in the high latitudes: using site-level data to evaluate Earth system models, *Biogeosciences*, 14, 5143-5169, 10.5194/bg-14-5143-2017, 2017.
- [Clark, M. P., Fan, Y., Lawrence, D. M., Adam, J. C., Bolster, D., Gochis, D. J., Hooper, R. P., Kumar, M., Leung, L. R., Mackay, D. S., Maxwell, R. M., Shen, C. P., Swenson, S. C., and Zeng, X. B.: Improving the representation of hydrologic processes in Earth System Models, \*Water Resour Res\*, 51, 5929-5956, 10.1002/2015wr017096, 2015.](https://doi.org/10.1002/2015wr017096)

- Comyn-Platt, E., Hayman, G., Huntingford, C., Chadburn, S. E., Burke, E. J., Harper, A. B., Collins, W. J., Webber, C. P., Powell, T., Cox, P. M., Gedney, N., and Sitch, S.: Carbon budgets for 1.5 and 2 degrees C targets lowered by natural wetland and permafrost feedbacks, *Nat Geosci*, 11, 568-+, 10.1038/s41561-018-0174-9, 2018.
- Ekici, A., Beer, C., Hagemann, S., Boike, J., Langer, M., and Hauck, C.: Simulating high-latitude permafrost regions by the JSBACH terrestrial ecosystem model, *Geosci. Model Dev.*, 7, 631-647, 10.5194/gmd-7-631-2014, 2014.
- Ekici, A., Chadburn, S., Chaudhary, N., Hajdu, L. H., Marmy, A., Peng, S., Boike, J., Burke, E., Friend, A. D., Hauck, C., Krinner, G., Langer, M., Miller, P. A., and Beer, C.: Site-level model intercomparison of high latitude and high altitude soil thermal dynamics in tundra and barren landscapes, *The Cryosphere*, 9, 1343-1361, 10.5194/tc-9-1343-2015, 2015.
- Elberling, B., Michelsen, A., Schadel, C., Schuur, E. A. G., Christiansen, H. H., Berg, L., Tamstorf, M. P., and Sigsgaard, C.: Long-term CO<sub>2</sub> production following permafrost thaw, *Nat Clim Change*, 3, 890-894, 10.1038/Nclimate1955, 2013.
- Fedorova, I., Chetverova, A., Bolshiyarov, D., Makarov, A., Boike, J., Heim, B., Morgenstern, A., Overduin, P. P., Wegner, C., Kashina, V., Eulenburg, A., Dobrotina, E., and Sidorina, I.: Lena Delta hydrology and geochemistry: long-term hydrological data and recent field observations, *Biogeosciences*, 12, 345-363, 10.5194/bg-12-345-2015, 2015.
- Gisnås, K., Westermann, S., Schuler, T. V., Melvold, K., and Etzelmüller, B.: Small-scale variation of snow in a regional permafrost model, *Cryosphere*, 10, 1201-1215, 10.5194/tc-10-1201-2016, 2016.
- Gochis, D.J., W. Yu, D.N. Yates, 2015: The WRF-Hydro model technical description and user's guide, version 3.0. NCAR Technical Document. 120 pages. Available online at: [http://www.ral.ucar.edu/projects/wrf\\_hydro/](http://www.ral.ucar.edu/projects/wrf_hydro/).
- Grant, R. F., Mekonnen, Z. A., Riley, W. J., Wainwright, H. M., Graham, D., and Torn, M. S.: Mathematical Modelling of Arctic Polygonal Tundra with Ecosys: 1. Microtopography Determines How Active Layer Depths Respond to Changes in Temperature and Precipitation, *J Geophys Res-Biogeophys*, 122, 3161-3173, 10.1002/2017jg004035, 2017.
- Hugelius, G., Strauss, J., Zubrzycki, S., Harden, J. W., Schuur, E. A. G., Ping, C. L., Schirmer, L., Grosse, G., Michaelson, G. J., Koven, C. D., O'Donnell, J. A., Elberling, B., Mishra, U., Camill, P., Yu, Z., Palmtag, J., and Kuhry, P.: Estimated stocks of circumpolar permafrost carbon with quantified uncertainty ranges and identified data gaps, *Biogeosciences*, 11, 6573-6593, 10.5194/bg-11-6573-2014, 2014.
- Knoblauch, C., Beer, C., Liebner, S., Grigoriev, M. N., and Pfeiffer, E. M.: Methane production as key to the greenhouse gas budget of thawing permafrost, *Nat Clim Change*, 8, 309-+, 10.1038/s41558-018-0095-z, 2018.
- Koven, C. D., Riley, W. J., and Stern, A.: Analysis of Permafrost Thermal Dynamics and Response to Climate Change in the CMIP5 Earth System Models, *J Climate*, 26, 1877-1900, 10.1175/Jcli-D-12-00228.1, 2013a.
- Koven, C. D., Riley, W. J., Subin, Z. M., Tang, J. Y., Torn, M. S., Collins, W. D., Bonan, G. B., Lawrence, D. M., and Swenson, S. C.: The effect of vertically resolved soil biogeochemistry and alternate soil C and N models on C dynamics of CLM4, *Biogeosciences*, 10, 7109-7131, 10.5194/bg-10-7109-2013, 2013b.
- Kumar, J., Collier, N., Bisht, G., Mills, R. T., Thornton, P. E., Iversen, C. M., and Romanovsky, V.: Modeling the spatiotemporal variability in subsurface thermal regimes across a low-relief polygonal tundra landscape, *Cryosphere*, 10, 2241-2274, 10.5194/tc-10-2241-2016, 2016.
- Kurylyk, B. L., Hayashi, M., Quinton, W. L., McKenzie, J. M., and Voss, C. I.: Influence of vertical and lateral heat transfer on permafrost thaw, peatland landscape transition, and groundwater flow, *Water Resour Res*, 52, 1286-1305, 10.1002/2015wr018057, 2016.
- Langer, M., Westermann, S., Muster, S., Piel, K., and Boike, J.: The surface energy balance of a polygonal tundra site in northern Siberia - Part 2: Winter, *The Cryosphere*, 5, 509-524, <https://doi.org/10.5194/tc-5-509-2011>, <http://www.the-cryosphere.net/5/509/2011/>, 2011a.
- Langer, M., Westermann, S., Muster, S., Piel, K., and Boike, J.: The surface energy balance of a polygonal tundra site in northern Siberia - Part 1: Spring to fall, *The Cryosphere*, 5, 151-171, <https://doi.org/10.5194/tc-5-151-2011>, <http://www.the-cryosphere.net/5/151/2011/>, 2011b.

- Langer, M., Westermann, S., Boike, J., Kirillin, G., Grosse, G., Peng, S., and Krinner, G.: Rapid degradation of permafrost underneath waterbodies in tundra landscapes-Toward a representation of thermokarst in land surface models, *J Geophys Res-Earth*, 121, 2446-2470, 10.1002/2016jg003956, 2016.
- Lawrence, D. M., and Slater, A. G.: A projection of severe near-surface permafrost degradation during the 21st century, *Geophys Res Lett*, 32, Artn L24401, 10.1029/2005gl025080, 2005.
- Lawrence, D. M., and Slater, A. G.: Incorporating organic soil into a global climate model, *Clim Dynam*, 30, 145-160, 10.1007/s00382-007-0278-1, 2008.
- Lawrence, D. M., Slater, A. G., and Swenson, S. C.: Simulation of Present-Day and Future Permafrost and Seasonally Frozen Ground Conditions in CCSM4, *J Climate*, 25, 2207-2225, 10.1175/Jcli-D-11-00334.1, 2012.
- Lawrence, D. M., Koven, C. D., Swenson, S. C., Riley, W. J., and Slater, A. G.: Permafrost thaw and resulting soil moisture changes regulate projected high-latitude CO<sub>2</sub> and CH<sub>4</sub> emissions, *Environ Res Lett*, 10, Artn 094011, 10.1088/1748-9326/10/9/094011, 2015.
- Lee, H., Swenson, S. C., Slater, A. G., and Lawrence, D. M.: Effects of excess ground ice on projections of permafrost in a warming climate, *Environ Res Lett*, 9, Artn 124006, 10.1088/1748-9326/9/12/124006, 2014.
- Li, D., Bou-Zeid, E., Barlage, M., Chen, F., and Smith, J. A.: Development and evaluation of a mosaic approach in the WRF-Noah framework, *J Geophys Res-Atmos*, 118, 11918-11935, 10.1002/2013jd020657, 2013.
- Liljedahl, A. K., Boike, J., Daanen, R. P., Fedorov, A. N., Frost, G. V., Grosse, G., Hinzman, L. D., Iijma, Y., Jorgenson, J. C., Matveyeva, N., Necsoiu, M., Reynolds, M. K., Romanovsky, V. E., Schulla, J., Tape, K. D., Walker, D. A., Wilson, C. J., Yabuki, H., and Zona, D.: Pan-Arctic ice-wedge degradation in warming permafrost and its influence on tundra hydrology, *Nat Geosci*, 9, 312-+, 10.1038/Ngeo2674, 2016.
- McGuire, A. D., Lawrence, D. M., Koven, C., Klein, J. S., Burke, E., Chen, G. S., Jafarov, E., MacDougall, A. H., Marchenko, S., Nicolsky, D., Peng, S. S., Rinke, A., Ciais, P., Gouttevin, I., Hayes, D. J., Ji, D. Y., Krinner, G., Moore, J. C., Romanovsky, V., Schaedel, C., Schafer, K., Schuur, E. A. G., and Zhuang, Q. L.: Dependence of the evolution of carbon dynamics in the northern permafrost region on the trajectory of climate change, *P Natl Acad Sci USA*, 115, 3882-3887, 10.1073/pnas.1719903115, 2018.
- Nitzbon, J., Langer, M., Westermann, S., Martin, L., Aas, K. S., and Boike, J.: Pathways of ice-wedge degradation in polygonal tundra under different hydrological conditions, submitted to *The Cryosphere*, 2018.
- Niu, G. Y., Yang, Z. L., Mitchell, K. E., Chen, F., Ek, M. B., Barlage, M., Kumar, A., Manning, K., Niyogi, D., Rosero, E., Tewari, M., and Xia, Y. L.: The community Noah land surface model with multiparameterization options (Noah-MP): 1. Model description and evaluation with local-scale measurements, *J Geophys Res-Atmos*, 116, Artn D12109, 10.1029/2010jd015139, 2011.
- Olefeldt, D., Goswami, S., Grosse, G., Hayes, D., Hugelius, G., Kuhry, P., McGuire, A. D., Romanovsky, V. E., Sannel, A. B. K., Schuur, E. A. G., and Turetsky, M. R.: Circumpolar distribution and carbon storage of thermokarst landscapes, *Nat Commun*, 7, ARTN 13043, 10.1038/ncomms13043, 2016.
- Painter, S. L., Moulton, J. D., and Wilson, C. J.: Modeling challenges for predicting hydrologic response to degrading permafrost, *Hydrogeol J*, 21, 221-224, 10.1007/s10040-012-0917-4, 2013.
- [Phoenix, G. K., and Bjerke, J. W.: Arctic browning: extreme events and trends reversing arctic greening, \*Global Change Biol\*, 22, 2960-2962, 10.1111/gcb.13261, 2016.](#)
- Qian, H. F., Joseph, R., and Zeng, N.: Enhanced terrestrial carbon uptake in the Northern High Latitudes in the 21st century from the Coupled Carbon Cycle Climate Model Intercomparison Project model projections, *Global Change Biol*, 16, 641-656, 10.1111/j.1365-2486.2009.01989.x, 2010.
- Qiu, C. J., Zhu, D., Ciais, P., Guenet, B., Krinner, G., Peng, S. S., Aurela, M., Bernhofer, C., Brummer, C., Bret-Harte, S., Chu, H. S., Chen, J. Q., Desai, A. R., Dusek, J., Euskirchen, E. S., Fortuniak, K., Flanagan, L. B., Friborg, T., Grygoruk, M., Gogo, S., Grunwald, T., Hansen, B. U., Holl, D., Humphreys, E., Hurkuck, M., Kiely, G., Klatt, J., Kutzbach, L., Langeron, C., Laggoun-Defarge, F., Lund, M., Lafleur, P. M., Li, X. F., Mammarella, I., Merbold, L., Nilsson, M. B., Olejnik, J., Ottosson-Lofvenius, M., Oechel, W., Parmentier, F. J. W., Peichl, M., Pirk, N., Peltola,

O., Pawlak, W., Rasse, D., Rinne, J., Shaver, G., Schmid, H. P., Sottocornola, M., Steinbrecher, R., Sachs, T., Urbaniak, M., Zona, D., and Ziemblinska, K.: ORCHIDEE-PEAT (revision 4596), a model for northern peatland CO<sub>2</sub>, water, and energy fluxes on daily to annual scales, *Geosci Model Dev*, 11, 497-519, 10.5194/gmd-11-497-2018, 2018.

[Reick, C. H., Raddatz, T., Brovkin, V., and Gayler, V.: Representation of natural and anthropogenic land cover change in MPI-ESM, \*J Adv Model Earth Sy\*, 5, 459-482, 10.1002/jame.20022, 2013.](#)

Rowland, J. C., and Coon, E. T.: From documentation to prediction: raising the bar for thermokarst research, *Hydrogeol J*, 24, 645-648, 10.1007/s10040-015-1331-5, 2016.

Schädel, C., Bader, M. K. F., Schuur, E. A. G., Biasi, C., Bracho, R., Capek, P., De Baets, S., Diakova, K., Ernakovich, J., Estop-Aragones, C., Graham, D. E., Hartley, I. P., Iversen, C. M., Kane, E. S., Knoblauch, C., Lupascu, M., Martikainen, P. J., Natali, S. M., Norby, R. J., O'Donnell, J. A., Chowdhury, T. R., Santruckova, H., Shaver, G., Sloan, V. L., Treat, C. C., Turetsky, M. R., Waldrop, M. P., and Wickland, K. P.: Potential carbon emissions dominated by carbon dioxide from thawed permafrost soils, *Nat Clim Change*, 6, 950-+, 10.1038/Nclimate3054, 2016.

Schuur, E. A. G., Bockheim, J., Canadell, J. G., Euskirchen, E., Field, C. B., Goryachkin, S. V., Hagemann, S., Kuhry, P., Laflour, P. M., Lee, H., Mazhitova, G., Nelson, F. E., Rinke, A., Romanovsky, V. E., Shiklomanov, N., Tarnocai, C., Venevsky, S., Vogel, J. G., and Zimov, S. A.: Vulnerability of permafrost carbon to climate change: Implications for the global carbon cycle, *Bioscience*, 58, 701-714, 10.1641/B580807, 2008.

Schuur, E. A. G., McGuire, A. D., Schadel, C., Grosse, G., Harden, J. W., Hayes, D. J., Hugelius, G., Koven, C. D., Kuhry, P., Lawrence, D. M., Natali, S. M., Olefeldt, D., Romanovsky, V. E., Schaefer, K., Turetsky, M. R., Treat, C. C., and Vonk, J. E.: Climate change and the permafrost carbon feedback, *Nature*, 520, 171-179, 10.1038/nature14338, 2015.

Seppälä, M.: Synthesis of studies of palsa formation underlining the importance of local environmental and physical characteristics, *Quaternary Res*, 75, 366-370, 10.1016/j.yqres.2010.09.007, 2011.

Sjöberg, Y., Coon, E., Sannel, A. B. K., Pannetier, R., Harp, D., Frampton, A., Painter, S. L., and Lyon, S. W.: Thermal effects of groundwater flow through subarctic fens: A case study based on field observations and numerical modeling, *Water Resour Res*, 52, 1591-1606, 10.1002/2015wr017571, 2016.

[Strauss, J., Schirrmeister, L., Grosse, G., Fortier, D., Hugelius, G., Knoblauch, C., Romanovsky, V., Schadel, C., von Deimling, T. S., Schuur, E. A. G., Shmelev, D., Ulrich, M., and Veremeeva, A.: Deep Yedoma permafrost: A synthesis of depositional characteristics and carbon vulnerability, \*Earth-Sci Rev\*, 172, 75-86, 10.1016/j.earscirev.2017.07.007, 2017.](#)

Viovy, N.: CRUNCEP Version 7 - Atmospheric Forcing Data for the Community Land Model. Research Data Archive at the National Center for Atmospheric Research, Computational and Information Systems Laboratory. <http://rda.ucar.edu/datasets/ds314.3/>, 2018.

Westermann, S., Langer, M., Boike, J., Heikenfeld, M., Peter, M., Eitzelmueller, B., and Krinner, G.: Simulating the thermal regime and thaw processes of ice-rich permafrost ground with the land-surface model CryoGrid 3, *Geosci Model Dev*, 9, 523-546, 10.5194/gmd-9-523-2016, 2016.

Zhang, T., Barry, R., Knowles, K., Heginbottom, J. and Brown, J.: Statistics and characteristics of permafrost and ground-ice distribution in the Northern Hemisphere I, *Polar Geography*, 23(2), 132-154, doi:10.1080/10889379909377670, 1999.